2016

Modeling Tropical Cyclone Storm Surge and Wind Induced Risk along the Bay of Bengal Coastline Using a Statistical Copula

Nazla Bushra
Louisiana State University and Agricultural and Mechanical College

MODELING TROPICAL CYCLONE STORM SURGE AND WIND INDUCED RISK ALONG THE BAY OF BENGAL COASTLINE USING A STATISTICAL COPULA

A Thesis

Submitted to the Graduate Faculty of the
Louisiana State University and
Agricultural and Mechanical College
in partial fulfillment of the
requirements for the degree of
Master of Science

in

The Department of Geography and Anthropology

by
Nazla Bushra
B.Sc., University of Dhaka, 2009
M.S., University of Dhaka, 2012
P.G. Dip., Bangladesh University of Engineering and Technology, 2013
May 2016

"Clouds come floating into my life,

no longer to carry rain or usher storm,

but to add color to my sunset sky."

— Rabindranath Tagore

All those colors are meaningful because you exist.
To my daughter Nawara Ishraq…….

ACKNOWLEDGMENTS

I convey my sincere heartiest gratitude and indebtedness to my advisor Dr. Jill C. Trepanier for her continued encouragement, supervision, contribution in using *R* programming and constant guidance throughout the course of this thesis work. Without her valuable direction and cordial assistance, it would have been very difficult to carry out this study under various constraints.

I would like to express my thanks to Dr. Robert V. Rohli and Dr. Barry D. Keim for their guidance to move forward very thoroughly. They each made numerous, valuable comments, and constructive criticisms. I thank them both for their continued encouragement throughout the course of this research work.

Special thanks are extended to Hal Needham for providing surge data and suggestions to complete the work successfully.

I am also grateful to the Almighty Allah for the successful completion of this thesis.

TABLE OF CONTENTS

LIST OF TABLES

LIST OF FIGURES

LIST OF ABBREVIATIONS

The following list of abbreviations are used throughout the thesis:

AIC	Akaike Information Criterion
BBS	Bangladesh Bureau of Statistics
BIDS	Bangladesh Institute of Development Studies
BMD	Bangladesh Meteorological Department
BoB	Bay of Bengal
BSISO	Boreal Summer Intraseasonal Oscillation
BUET	Bangladesh University of Engineering and Technology
CCS	Centre for Climate and Safety
CDF	Cumulative Density Function
CEGIS	Center for Environmental and Geographic Information Services
CICFRI	Central Inland Capture Fisheries Research Institute
GOB	Government of the People's Republic of Bangladesh
GPI	Genesis Potential Index
IBTrACS	International Best Track Archive for Climate Stewardship
IMD	Indian Meteorological Department
ISO	Intraseasonal Oscillation
JTWC	Joint Typhoon Warning Center
MJO	Madden-Julian Oscillation
MoEF	Ministry of Environment and Forest
NCAR	National Center for Atmospheric Research
NCDC	National Climate Data Center
NHC	National Hurricane Center
NIO	North Indian Ocean
NOAA	National Oceanic and Atmospheric Administration
RSMC	Regional Specialized Meteorological Centre
SAARC	South Asian Association for Regional Cooperation
SMRC	SAARC Meteorological Research Centre
SST	Sea Surface Temperature
SURGEDAT	Surge Database
TC	Tropical Cyclone
WMO	World Meteorological Organization

ABSTRACT

High winds, torrential rain, and storm surges from tropical cyclones cause massive destruction to property and cost the lives of many people. Among the coastal areas affected by these major natural calamities, the coastline of the Bay of Bengal (BoB) ranks as one of the most susceptible to tropical cyclone storm surge risk due to its geographical setting and population density, Bangladesh suffers the most. The purpose of this study is to describe the relationship between storm surge at the BoB and peak reported wind and describe the dependency structure between wind speeds and storm surges at that location. Various models have been developed to predict storm surge in this region but none of them quantify statistical risk with empirical data. This research demonstrates a methodology for estimating the return period of the joint hazard based on a bivariate copula model. An Archimedean Gumbel copula with Weibull and normal margins is specified for the result the coast of BoB can expect a cyclone with peak reported winds of at least 24 m s^{-1} and surge heights of at least 4.0 m, on average, once every 3.2 years (2.7–3.8). The BoB can expect peak reported winds of 62 m s^{-1} and surge heights of at least 8.0 m, on average, once every 115.4 years (55.8–381.1). In this ocean basin, surge heights are comparably higher when compared to other ocean basins. Application of the copula will mitigate future threats of storm surge impacts on coastal communities of the BoB.

CHAPTER 1.
INTRODUCTION

1.1 Tropical Cyclones and Storm Surge Risk over the Bay of Bengal

Tropical cyclones (TCs), with the associated high winds, torrential rain, and storm surge at landfall, are one of Earth's most destructive natural phenomena. These characteristics cause massive destruction to property, coastal structures, and agriculture (Alam and Collins 2010, Islam et al. 2011, Mallick et al. 2011). The events are so extreme they can cost the lives of many people living at or near coastal regions (Alam and Collins 2010, Islam et al. 2010). These events create economic losses every year to affected countries, which is mainly the result of violent winds and deep storm surges (Rao et al. 2007). TCs form over warm ocean surfaces with sea-surface temperatures (SST) > 26°C; low magnitude vertical wind shear; larger than normal low-level vorticity; and higher than normal mid-troposphere relative humidity (Sahoo and Bhaskaran 2015). The nature of the ocean basin, including the continental shelf and the tidal conditions during the TC landfall, along with high population density, increases risk from TCs due to storm surge inundation. Storm surge is defined as an unusual increase in water level caused by a storm, over and above the predicted astronomical tides (National Hurricane Center 2015). Risk assessment and warning systems can be improved by better understanding the geophysical settings and the TC characteristics in a given ocean basin.

Among the coastal areas affected by these major natural calamities, the coastline of the Bay of Bengal (BoB) ranks as one of the most susceptible to TC storm surge risk due to its geographical setting and population density (Chan 2014), as well as the size of the surges, which are the largest in the world (Needham et al. 2015). Cyclone tracks are steered by the semi-enclosed and funnel shape nature of this basin. The BoB is

historically significant for receiving the most catastrophic, deadly cyclones with death tolls at the top of all records (Sahoo and Bhaskaran 2015). Among the countries that share the BoB coastline, Bangladesh is the most vulnerable based on the number of landfalls since 1970 (Dube et al. 1997; IMD 2010; SURGEDAT 2015). Hence, there is a need to understand TC extreme winds, storm surges, and associated coastal inundation in this part of the world.

To achieve greater confidence, assess the risk of storm surge and extreme winds in the BoB, studies of its physical and dynamic characteristics are needed. Various models have been developed to predict storm surge in this region (Das 1972; Johns and Ali 1980; Ghosh et al. 1983; Dube et al. 1985, 2000a, 2000b, 2004, 2006; Abrol 1987; Katsura et al. 1992; Sinha et al. 1996, 2008; Roy et al. 1999; Jain et al. 2006; Rao et al. 2009), but none of them quantify statistical risk with empirical data for this region of the world. Chu and Wang (1998), Emanuel et al. (2006), Elsner et al. (2008), Liu et al. (2009), Lin et al. (2010), Irish et al. (2011), and Trepanier et al. (2015) quantify risk with empirical data but not in the BoB.

1.2 Research Question

Due to the devastating nature of TCs and high population density along the BoB coast, it is important to quantify risk of storm surge and wind events for emergency managers. This study uses a statistical model to estimate the risk of extreme wind speeds and TC-induced storm surges in the BoB. A statistical copula model is used to model TC characteristics incorporating peak wind speed and surge height data. This model will estimate the combined statistical risk of wind speeds and storm surges along this coast. This study will focus on the following question:

- What is the risk of experiencing a combined extreme wind and storm surge from a TC along the BoB coastline?

To answer this question, the objective of the study is to quantify the probability of occurrence of specific wind speed and storm-surge magnitudes over time. This provides combined risk of cyclone wind and surge at the coast of BoB at different temporal scale.

1.3 Hypothesis

Due to the funnel-shaped coastline, the gentle gradient of the continental shelf, and evidence from the historical records, the BoB has a high probability of a combined extreme wind and surge event. The severity of the surge's impacts may depend on time of occurrence, local factors, and the use of a warning system.

1.4 Study Area

In the Northern Hemisphere, the Indian Ocean Basin is divided into two divisions: the BoB and the Arabian Sea (AS). The BoB experiences more cyclone occurrences than the AS (Paul 2009). This research focuses on TCs originating over the Indian Ocean, following the path over the BoB, and making landfall over the coasts of Bangladesh, Sri Lanka, the east coast of India (West Bengal, Orissa, Andhra Pradesh, and Tamil Nadu), and the west coast of Myanmar. Landfall is defined as the eye of the storm passing over a coastline. The BoB is the northeast horn of the Indian Ocean, and Bangladesh is at the northern edge of that triangular horn (Figure 1.1). The BoB lies roughly within 5°N to 22°N latitude and 80°E to 90°E longitude. This large but relatively shallow embayment occupies an area of about 2,173,000 km^2 (839,000 mi^2) and is about 1,600 km (1,000 miles) wide, with an average depth of more than 2,600 m (8,500 ft) (Morgan 2015).

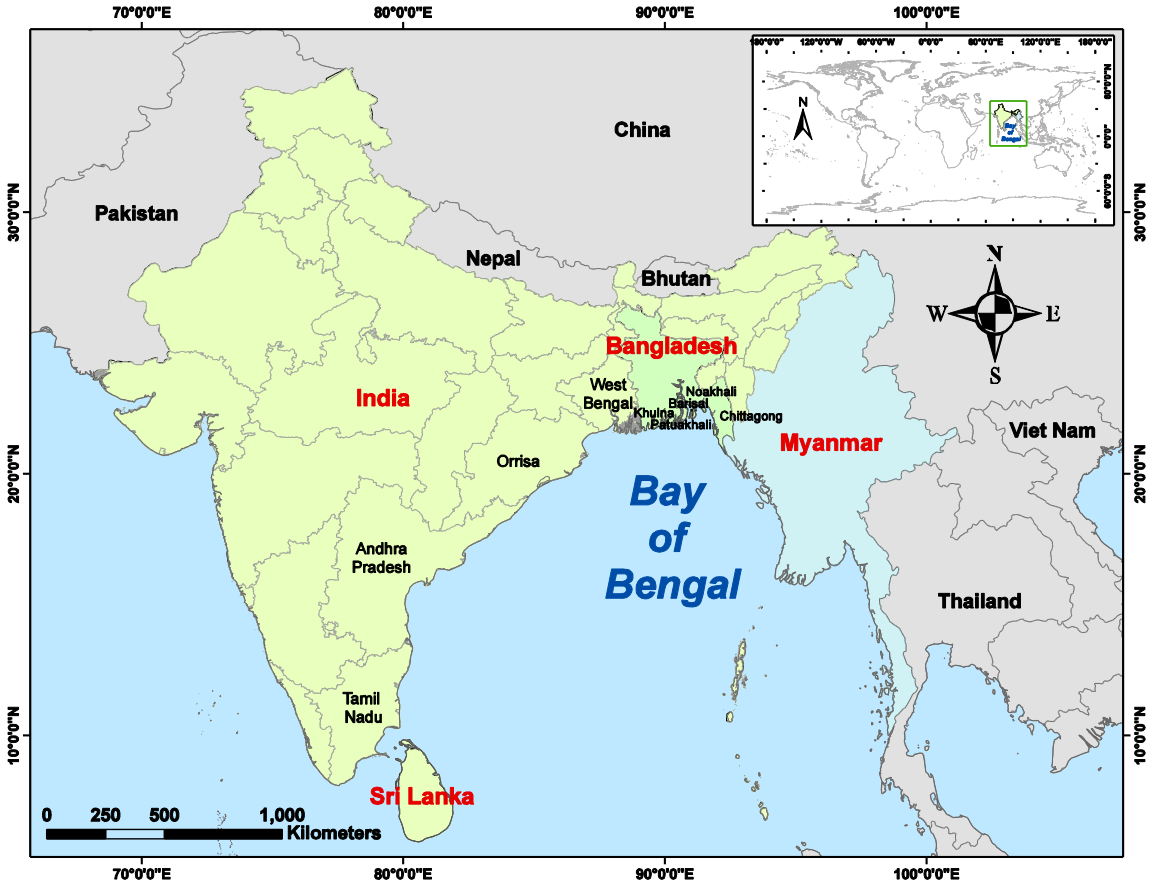

Figure 1.1 – Study area: the Bay of Bengal. An inset map is included to show the global location of the study area

The BoB coast extends from Kanniyakumari (Tamil Nadu, India) in the southwest to Kawthuang (Myanmar) in the southeast. The coastal expanse is 5,055 km long and covers all the coastlines mentioned above except Sri Lanka, which has about 1340 km of coastline (CICFRI 2004). The climate of the region is subtropical to tropical and is characterized by high temperatures and medium precipitation, with virtually all precipitation falling as rain during the Southwest Monsoon (June to September), causing a drastic decline in salinity in the BoB (Central Inland Capture Fisheries Research Institute 2004). According to the Central Inland Capture Fisheries Research Institute (2004) in West Bengal, India, the reported annual sea surface temperature of the BoB varies within a narrow range of 27 to 29°C. This makes it a prime location for TCs.

1.5 Overview

This introduced the TC and storm surge risk over the BoB coastal region. The research question and hypothesis are identified, followed by a general description of the study area. Chapter Two is a complete literature review on storm surge and wind-induced risk at the BoB coastline. The literature review highlights the necessity for quantifying statistical risk of TC storm surge and wind for emergency managers.

Chapter Three discusses the data and methods required to create the copula for risk modeling. Chapter Four presents and discusses the results. Chapter Five provides the conclusions, limitations to the current model, and recommendations for future work.

CHAPTER 2.
LITERATURE REVIEW

This chapter provides a background for TCs and storm surge risk in the BoB, with a specific focus on the coastline of Bangladesh.

2.1 Tropical Cyclones

The Indian Meteorological Department (IMD) defines a TC as a rotational low pressure system in the tropics with a central pressure of at least 5hPa less than the surrounding area and a minimum sustained wind speed of 17.22 m s^{-1} (62 km hr^{-1}or 34 knots) (IMD 2010; Akter and Tsuboki 2014). These vast, violent whirls of air span 150 to 800 km in size and spiral around a center as they progress along the sea surface at a rate of 300 to 500 km day^{-1} (IMD 2010).

The spatiotemporal distribution of SST exceeding 26°C and the location of the monsoon trough (monsoon-type intertropical convergence zone) are primary factors explaining the seasonal distribution and frequency of TCs over the oceans (McBride 1995). Cyclone formation in all ocean basins is also correlated with the seasonally averaged values of six parameters (Gray 1975, 1979): of the six parameters, there are three dynamic variables (low-level relative vorticity, inverse of the tropospheric vertical wind shear, and the Coriolis parameter) and three thermodynamic variables (ocean thermal energy extending to a sufficient depth, moist static instability, and mid-tropospheric relative humidity). When environmental conditions are favorable, an external wind burst into regions already containing a tropical disturbance can trigger TC formation (i.e., cyclogenesis) by causing development of deep convection (Zehr 1992; Gray 1998). This can subsequently evolve into a TC vortex capable of self-intensification.

A fully developed TC has a central cloud free region of calm winds, known as the eye of the cyclone, with a diameter varying from 10 to 50 km (IMD 2010). Surrounding the eye is a dense wall of clouds, called the eyewall, characterized by very strong winds and torrential rains with a width from 10 to 150 km (IMD 2010). Wind speeds gradually decrease away from the core region, which eventually terminate over areas of weaker winds with overcast skies and the occasional thunderstorm. There may be one or more rain bands in a cyclone where higher rainfall occurs (IMD 2010).

2.1.1 Tropical Cyclones in the Bay of Bengal

TCs are common phenomena in the BoB and influence every country with a North Indian Ocean (NIO) coastline (east coast of India, Sri Lanka, Bangladesh, and Myanmar). About one quarter of the world's population resides in the countries sundering the BoB, approximately 400 million of whom live in the Bay's catchment area (Hossain 2004). Between 1891 and 1998, 178 devastating cyclones with wind speeds exceeding 24.17 m s^{-1} (87 km hr^{-1}) formed in the BoB and were responsible for millions of human lives lost and the destruction of vast amounts of natural resources and property (BUET and BIDS 1993; Shrestha et al. 1998). Although only a few storms form in this region every year, the events seem to be deadlier than elsewhere, with 80−90 percent of global casualties happening along the BoB coastline for many years after the 1950s (Chowdhury 2002; Debsarma 2009; Jia 2013).

The BoB is one of the world's most active zones for tropical cyclogenesis (Paul 2009). In contrast to the other ocean basins, where environmental conditions are most favorable for TCs in late summer (Neumann 1993), the NIO has a bimodal peak in TC activity with one occurring in May and the other in November (Akter and Tsuboki 2014).

Most cyclones form within the regional monsoon trough; thus, their seasonal distribution has been related to the migration of the monsoon trough over the ocean (McBride 1995).

The high cyclogenesis potential in the BoB results from combined forcing of seasonal (Akter and Tsuboki 2014) and intraseasonal environmental conditions (Kikuchi and Wang 2010). Kikuchi and Wang (2010) found a statistical relationship between NIO TC genesis and two intraseasonal oscillation (ISO) modes - the Boreal Summer Intraseasonal Oscillation (BSISO), which propagates primarily northward, and the Madden-Julian Oscillation (MJO), which propagates eastward. Both ISO modes favor TC genesis by causing a synoptic-scale disturbance at least six days prior to TC formation in the NIO (Akter and Tsuboki 2014). Kikuchi and Wang (2010) reported that over 70% of ISO-related cyclogenesis was associated with the BSISO in May–June and September–November, with the rest associated with the MJO in November–December.

Consistent with the findings of Kikuchi and Wang (2010), Yanase et al. (2012) assessed cyclogenesis over the NIO in relation to the Genesis Potential Index (GPI). Active cyclogenesis was associated with a strong northward-moving GPI signal with a periodicity of approximately 30–40 days associated with the BSISO. They attributed the strong GPI during the BSISO to abundant relative humidity and large absolute vorticity within its convective phase (Yanase et al. 2012). In the BoB, northward propagating BSISO enhances cyclones more than MJO.

Both the seasonally varying monsoon trough position and the intraseasonal ISO phase allow the tropical disturbances over the NIO to develop further into TCs. In the BoB, the coasts of Sri Lanka and Myanmar are less affected by TCs in comparison with the coasts of Bangladesh and India (Murty and Flather 1994, Shaji et al. 2014). This is due to

the monsoon trough position, north-east trade wind and counter trade winds position and intraseasonal ISO condition, and also possibly due to geographic orientation of the coasts.

2.1.2 Storm Surges in the Bay of Bengal

Of the TCs that cause at least 5000 casualties worldwide, 53% occur in Bangladesh making it one of the world's most vulnerable countries to TCs (Ali 1999; UNDP 2004). About 10% of the TCs in the world originate in the BoB, and one-sixth of these make landfall on the coast of Bangladesh (Islam et al. 2011). About 41% of these cyclones travel through funnel-shaped central region each year, which makes the central coast of Bangladesh vulnerable to storm surge (Paul and Rahman 2006). A cyclone with a high potential for damage, for example having high winds, may not be devastating depending on its time of occurrence, local factors, and natural and human adaptation capability. In Bangladesh, TC events typically result in high loss of life and economic damage because of the combination of geographic location, topography, population density, levels of poverty, and extraordinarily large storm surges (CCS 1991; Murty and El Sabh 1992; Jia 2013). The funnel-shaped coastline, shallow coastal water, favorable cyclone track, and innumerable inlets including the world's most populated river system (the Ganges-Brahmaputra-Meghna) put this low-lying region under high TC storm surge risk (Ali 1979; Dube et al. 2009; Khan and Damen 2013).

Storm surge from a TC is an unusual increase in water level caused by a storm, over and above the predicted astronomical tides (National Hurricane Center 2015). The term storm tide is also often used to describe storm surge. Storm tides are the total undulation of waters due to tidal fluctuations in addition to the weather event, and often exist for a few days (Murty 1984). Thus, removal of astronomical tides from storm tides defines the actual

storm surge height generated from a storm. Storm surge is a very complex phenomenon because it is sensitive to the slightest changes in storm intensity, forward speed, size (radius of maximum winds-RMW), angle of approach to the coast, central pressure (minimal contribution when considering wind), width and slope of the ocean bottom, and shape and characteristics of coastal features such as bays and estuaries (National Hurricane Center 2015). Approximately 62% of Bangladeshi coastal land has an elevation less than 3 m and 86% lies below 5 m (CEGIS 2009; Jia 2013). Moreover, Bangladesh has 710 km of coastline exposed to the BoB, which is relatively long compared to the size of the country (Jia 2013).

In Bangladesh, severe cyclones in 1584, 1737, 1876, and 1897 took a combined 914,000 casualties (MoEF 2009). In the past 50 years, around 718,000 lives in Bangladesh have been lost during such cyclones (Haque et al. 2012). Of the 718,000 lives lost, 70% occurred in only a single storm in 1970 called the Bhola Cyclone which claimed some 500,000 lives (Choudhury 2002). In recent decades, super cyclones (with wind speeds of > 61 m s^{-1}) have occurred in 1970, 1991, and 2007, leading to huge losses of life and property (Khalil 1992; GOB, European Commission and World Bank 2008) (Table 2.1). Cyclone Sidr's (2007) monetary losses totaled US $1.67 billion (GOB 2008) and the 1991 cyclone caused about US $2.4 billion (Kausher et al. 1996) in material damage. Table 2.2 shows cyclone severity, surge height, wind speed, and deaths in Bangladesh for major cyclone events from 1960–2007.

Authorities in Bangladesh have drastically improved the pre-, during-, and post-disaster management strategies in the past three decades (Alam and Collins 2010). This largely includes infrastructure developments, cyclone warning systems, and

communication to raise awareness among the local population (Khan 2008). These initiatives reduced the death rate for severe cyclones in recent years (Table 2.2).

Table 2.1 − Comparison of the three most devastating cyclones in Bangladesh over recent decades (Khalil 1992; GOB, European Commission and World Bank 2008)

Year of Occurrence	1970 Bhola Cyclone	1991 Chittagong Cyclone	2007 Cyclone Sidr
Wind Speed (km hr^{-1})	66.94	53.61	66.67
Storm Surge Height (m)	10	5	6
Death of People	About 500, 000	About 150,000	About 4,000

Table 2.2 − Cyclone severity according to Indian Meteorological Department (IMD) scale and deaths in Bangladesh 1960–2010 *(Karmakar 1998; Dasgupta et al. 2010; SURGEDAT 2015)

Year	Number of deaths	Peak wind speed m s^{-1} (km hr^{-1})	Storm tide (m)	Severity index
1960	8119	58 (210)	9.1	5
1961	11466	41 (146)	8.8	5
1963	11520	56 (203)	9.1	5
1965	20152	58 (210)	5.8	5
1966	850	41 (146)	9.6	5
1970	500300	67 (241)	9.1	6
1973	183	34 (122)	5.1	5
1974	50	45 (162)	5.3	5
1985	11069	43 (154)	4.5	5
1988	9590	45 (162)	3.3	5
1997	410	62.5 (225)	5	6
2007	4234	67 (240)	5.75	6

*Storm tides come from Karmakar (1998) and SURGEDAT (2015) and peak wind speed and number of death come from Dasgupta et al. (2010).

The documents used as sources for Table 2.2 follow the “cyclone severity index” of the IMD based on wind intensity to compile the severity index. The categories of the IMD damage potential scale or severity index of different cyclone systems are broken up based on expected damage to the landscape. The low severity has minimal damage (for example, minor damage to structures, agricultural lands, embankments; breaches in road due to flooding) and high severity has total destruction (for example, extensive damage to

buildings, structures, and roads; uprooting of poles; total disruption of agricultural land, communication and power supply; submerging of coastal lands due to flooding and sea water inundation).

Yet even with the improved hazard mitigation strategies, physiographic features, location factors, and demographic and economic conditions all suggest that Bangladesh remains the world's most vulnerable country to TC storm surge.

2.2 Tropical Cyclone Risk Modeling

Historical records of different variables are incorporated in cyclone risk modeling studies to make meaningful estimations of cyclone risk. Wind speeds and storm surges are major elements in many risk models. The following sections describe univariate risk models, first for wind and then for storm surge. Modeling a combined risk is discussed subsequently.

2.2.1 Wind Speed Risk Modeling

The historical record of TC wind intensities spanning back over the last 100 years is relatively robust and provides evidence that damage and loss of life results mostly from cyclone induced winds and storm surges (Emanuel et al. 2006). This evidence has motivated several efforts to assess risks associated with TC winds. Huang et al. (2001) and Watson and Johnson (2004) have provided a comprehensive review of wind loss modeling. Though a significant number of studies have been done on TCs at the BoB, none of them addressed the cyclone wind risk in the region directly and comprehensively.

In early wind risk assessment studies, statistical distributions such as the log-normal distribution (Georgiou et al. 1983) and the Weibull distribution (Neumann 1987) were used to model the behavior of TC winds. Empirical models were applied (Georgiou 1985), as

well as inferential models (Darling 1991, Chu and Wang 1998). Murnane et al. (2000) used a cumulative probability distribution function to infer global estimates of hurricane actual (rather than relative) wind intensity.

TC key parameters such as central pressure (Vickery et al. 2000a, 2009; Emanuel et al. 2006), the radius to maximum winds (Vickery et al. 2009), the heading (Vickery et al. 2000a, 2009), translation speed (Vickery et al. 2000a, 2009), position of the storm (Emanuel et al. 2006, Lee and Rosowsky 2007), maximum wind speed (Chu and Wang 1998, Vickery et al. 2009), changes in wind direction (Lee and Rosowsky 2007), intensity along each track (Vickery et al. 2000b, Emanuel et al. 2006), and sea surface temperature (Emanuel 1988, Vickery et al. 2000a, 2000b) are the most common variables used in the statistical modeling for the TC wind risk estimation. Huang et al. (2001) define the long-term TC risks on the basis of statistical extreme wind climate. Harper (1999) describes simulation techniques to provide essential insight into the complex mechanisms that underscore extreme winds in a region and provide a reasonable basis for extrapolation to very long return periods.

Vickery and Twisdale (1995) describe the rate of decay of the TC after landfall with two key components of a TC simulation process: the wind-field model and the filling model. Vickery and Twisdale (1995) predicted hurricane wind speeds in the United States. This study provided an updated hurricane simulation methodology incorporating newly developed wind-field and filling models to obtain hurricane wind speeds associated with various return periods along the hurricane-prone coastline of the United States.

Vickery et al. (2000b) solved the nonlinear solution to the equations of motion of a hurricane and then parameterized it for use in fast-running simulations. The model

considered the effects of changing sea surface roughness and the air-sea temperature difference on the estimated surface-level wind speeds. Comparisons between modeled and observed hurricane wind speed records showed that the model provides a good representation of the hurricane wind field. Vickery et al. (2000b) introduced a new simulation approach from statistics where by the entire track (before and after landfall) of a tropical storm in the Atlantic Basin can be modeled for hurricane wind risk analysis over large regions; whereas traditional simulation models required selection of a subregion from which statistical distributions had been derived. Vickery et al. (2009) updated the hurricane simulation model to form a basis of hurricane wind speed to analyze hurricane wind speed risk and uncertainty.

Thompson and Cardone (1996) recreated hurricane surface winds in relation to ocean waves and surge in a discrete numerical wind field model. Emanuel et al. (2006) estimated hurricane wind risk with a coupled ocean-atmosphere model; he computed hurricane tracks and combined a deterministic numerical approach with statistical track generation from a probability density function to simulate storm intensity.

2.2.2 Storm Surge Risk Modeling

Models associated with storm surge predict probable storm and landfall locations, peak surge amplitudes along the coast, and inland inundation associated with storm surges (Azam et al. 2004, Dube et al. 2009, Lewis et al. 2013). In the context of storm surge risk in this study, risk refers to the statistical likelihood of the surges affecting a given location or region (Trepanier et al. 2015). An estimation of occurrence of storm surges or storm frequencies in a specific area provides an assumption of the risk over the entire study region.

Previous studies with numerical models suggest that the coastline of the BoB is susceptible to storm-surge inundation, with the magnitude varying with consequent tidal conditions and associated wind speeds. Das (1972), Johns and Ali (1980), Ghosh et al. (1983), Dube et al. (1985, 2000a, 2004, 2006), Abrol (1987), Katsura et al. (1992), Sinha et al. (1996, 2008), Roy et al. (1999), Jain et al. (2006), and Rao et al. (2009) have developed numerical storm surge prediction models applied in the BoB. At first, numerical models only focused on synoptic scale prediction to estimate storm-surge amplitude (Dube et al. 2009). Gradually the model foci turned to operational numerical storm surge prediction (Dube et al. 1994, 1997, 2000a, 2004, 2005, 2006; Rao et al. 1997; Chittibabu 1999; Chittibabu et al. 2002; Jain et al. 2006), real-time storm surge prediction (Dube et al. 1994, 2004; Dube and Gaur 1995; Chittibabu et al. 2002; Jain et al. 2006), and high-resolution location-specific models for accurate prediction of the surge (Dube et al. 1994, 2000b, 2004; Rao et al. 1997; Chittibabu 1999; Chittibabu et al. 2002; Jain et al. 2006). Chu and Wang (1998), Emanuel et al. (2006), Elsner et al. (2008), and Lin et al. (2010) at the Atlantic and Pacific coasts of the U. S., Liu et al. (2009) at the coast of China, and Irish et al. (2011) and Trepanier et al. (2015) at the coast of the Gulf of Mexico applied statistical storm surge risk models to predict storm surge risks at those coasts. The models are significant for early warning systems, emergency management, and to investigate multiple forecast scenarios.

2.3 Combined Tropical Cyclone Risk Modeling

In the above sections emphasis has been given on single variable cyclone wind risk and storm surge risk modeling. Now a discussion of combined, or multivariate, risk modeling is presented.

Numerical models depend on various inputs of oceanographic and meteorological variables (Dube et al. 2009). Computationally intensive numerical models involve a large number of input parameters which include water level, sea level variations, wave heights, wind velocity, bathymetry, topographic undulation, landscape variability, historical data, simulated data, and others (Jia and Taflanidis 2013). Numerical models compare model predictions with the observational surge level. In 1977 at the Andhra Coast and, in 1982 at the Orissa Coast, numerical models were used to predict the combined tidal and surge response by using respective tide-gauge reading and inland flooding (Johns et al. 1985).

On the other hand, statistical modeling uses real-time observed data and known statistical theories to model TC behavior. Statistical models are used to represent hypotheses or assumptions depending on the observed data. Statistical models are constrained by the known limits of the data and the theory, which has the potential of making them reliable sources to model TC behavior.

Emanuel et al. (2006) contributed significant knowledge to study of hurricane risk using both statistical and numerical approaches. The researchers ran two individual models with one model using empirical data to assess the hurricane positions and other model using the predicted data to estimate storm wind magnitude (Emanuel et al. 2006). Today, extensive availability of data related with hurricane risk assessment has provided the opportunity to make meaningful estimates of the risk using a combine numerical statistical approach (Emanuel et al. 2006). The authors also emphasize that recently all numerical estimation techniques begin with compilations of all observed data as they are readily available and give more accurate results; but for the places where the data records are sparse and locally unavailable the task becomes more complicated (Emanuel et al. 2006).

2.3.1 Joint Probability Modeling

Research is increasing in the area of probability and statistics, in which multivariate models are analyzed with various types of dependence structures (Joe 1997). Dependence structures can be explained under joint probability distribution. The joint probability distribution for two or more variables that are defined on a probability space gives the probability that each of those variables falls in any particular range or discrete set of values specified for that variable. The joint probability distribution can be expressed in terms of a joint cumulative distribution function or joint probability density function (continuous variables) or joint probability mass function (discrete variables). These in turn can be used to find two other types of distributions: the marginal distribution and the conditional probability distribution (Hazewinkel 2001). For the joint probability density function for continuous multivariate distributions, the univariate marginals and the multivariate or dependence structure can be separated and the multivariate structure can be represented by a copula (Joe 1997).

2.3.2 Copula Modeling

A copula is a function or tool that links univariate marginals to their full multivariate distribution (Frees and Valdez 1998). According to Sklar's theorem any multivariate joint distribution can be written in terms of univariate marginal distribution functions and a copula, which describes the dependence structure between the variables (Nelsen 1998). The joint distribution function expresses the fact that copulas embody the way in which multidimensional distribution functions are coupled to their 1-dimensional margins, and also the way in which random variables defined over a common probability space are connected or linked together (Sklar 1973). If G is an n-dimensional joint distribution

function with 1-dimensional margins *F1,..., Fn,* then there exists a function *C* (called an "*n-copula*") from the unit *n*-cube to the unit interval such that

$$G(x_1, ..., x_n) = C(F_1(x_1), ..., F_n(x_n))$$ for all real *n*-tuples $(x_1, ..., x_n)$.

Multivariate distributions share the necessary conditions in a joint distribution function over the probability space. Multivariate distributions in a joint probability distribution function originate from the same existing environment that the consequences can be explanatory under same criteria with univariate margins. For example, in this study cyclone wind speed and storm surge are the consequences of the same storm event originating from ocean-air interaction and their dependence structure can be explained by a copula.

Trepanier et al. (2015) used a statistical copula model to estimate the combined surge and wind risk from hurricanes at Galveston, Texas. The researchers came up with precise results of storm surge and wind risk, which is computed from the long term observed data of wind speed and surge height, without any complex intensive computations. This model could be improved by including additional variables. But if additional variables are not available or rather the copula itself is suited to create just its bivariate approach that can essentially model the risk estimate of those two variables dependent on each other but independent on the entire basin itself. Copula allows the capacity to model empirical relationships between observed data as separate entities from the additional data and to pin point a relationship between two variables at a specific location. As storm surge risk analysis involves data of different types, such as oceanographic, meteorological, hydrological, bathymetric, and coastal geometric, it is obvious that all these data cannot always be available to run a complete model. As a result, there are few studies

using observed data in storm surge risk analysis in the BoB, in comparison to modeled data in this region (Dube et al. 2009).

Among various statistical models, a copula is a straight-forward method that becomes a valuable alternative to the more commonly used multivariate methods in climate research, in which non-normally distributed random climatic data are involved (Schölzel and Friederichs 2008). The climate system is a complex, high-dimensional, and nonlinear system, and it is difficult to characterize using univariate components (Schölzel and Friederichs 2008). Instead, the climate system tends to be composed of a suite of variables that together approach a probability distribution of multivariate random variables (Schölzel and Friederichs 2008), making it ideally suited to copula modeling. In storm surge risk analysis, most of the previous model studies are limited by their reliance on a univariate component of storm surge (Chu and Wang 1998; Elsner et al. 2008; Lin et al. 2010; Irish et al. 2011). In contrast, recent studies based on copula (Liu et al. 2009; Trepanier et al. 2015) facilitate the analysis of risk contributed by multivariate random variables.

Depending on data availability, a copula model can be expanded to incorporate more variables and spatial extensions than have been incorporated in previous TC research. According to Schölzel and Friederichs (2008), three typical situations of bivariate random variables are considered in a copula framework: (1) the same climate variable at different locations, (2) different climate variables at the same location, and (3) bivariate extremes, as far as they can be expressed in the copula framework.

Copulas were introduced by Sklar (1959). The technique has become popular in recent decades, especially in the fields of econometrics (Embrechts et al. 2003), finance (Breymann et al. 2003), risk management (Schölzel and Friederichs 2008), insurance (Haas

1999), and more recently in hydrology (Renard and Lang 2007; Genest et al. 2007; Bardossy and Li 2008). Copula modeling has recently become more prominent in climate research as it is able to analyze risk more efficiently within a holistic climatic framework. Bivariate frequency analysis of observed and simulated storm events (Vandenberghe et al. 2011), analysis of precipitation extremes (Zhang et al. 2012), risk evaluation of drought (Zhang et al. 2013), and analysis of risk from hydrodynamic boundary conditions (Wahl et al. 2012) are some examples of copula modeling applied in climate research. This research capitalizes on the advantages of copula modeling of wind speed and storm surge risk analysis in the BoB, where it has not been implemented in previous research.

CHAPTER 3.
DATA

3.1 Data

This research utilizes peak storm surge and cyclone wind speed data along the coast of the BoB. The data have been collected mainly from the South Asian Association for Regional Cooperation (SAARC) Meteorological Research Centre (SMRC), the world's storm surge data center (SURGEDAT), and the International Best Track Archive for Climate Stewardship (IBTrACS). The rest of the data have been collected from various journals and reports. For storm surge, peak height at or near landfall has been considered, and for wind speed, the reported peak wind and winds prior to landfall have been considered. For this study, 64 records have been collected pairing surge with reported peak wind and pre-landfall winds.

Two distinct datasets of wind and surge pairs are used for analysis. Each event has one wind and one storm surge pair associated with it. The first, called dataset 1 (DS1), considers the reported peak wind speed and storm surge given from the SMRC with the storm surge data supplemented by SURGEDAT and wind data supplemented by IBTrACS. The second (DS2) considers the 12-hour pre-landfall wind speed reported from IBTrACS with the same storm surge data in the first set. The reasoning for this is detailed below. First, the storm surge data are described and, second, the rationale and description of the two wind data sets are given.

3.1.1 Storm Surge

The South Asian Association for Regional Cooperation (SAARC) Meteorological Research Centre (SMRC) provided data for 37 storm surge events for this study from 1942–1997. The SMRC is a research center monitoring meteorological phenomena consistent

with SAARC Member States (Afghanistan, Bangladesh, Bhutan, India, Maldives, Nepal, Pakistan, and Sri Lanka). The SMRC accumulates data from various publications of the Bangladesh Meteorological Department (BMD), the Indian Meteorological Department (IMD), newspapers, journals, and reports. In SMRC, storm surges height includes the combined effect of the storm tide and astronomical tide (Karmakar 1998). The data provided include the peak storm surge height in meters along with a qualitative description of location. To quantify the location given, estimation of latitudes and longitudes have been made using landfall location given by the SMRC, cyclone track information from IBTrACS, and by applying theoretical knowledge of hurricane structure which suggests the largest storm surge occurs at the right-forward quadrant of the storm in the Northern Hemisphere (NOAA 2015).

The global storm surge database SURGEDAT provided an additional 17 surge events from 1885–2011 (Needham et al. 2013). These data include the peak water level and the latitude and longitude of the record. SURGEDAT retrieved data from numerous academic publications, Unisys Weather (Unisys Corporation 2015) and the Joint Typhoon Warning Center (JTWC). Most of the storm surge heights in SURGEDAT indicate the combined effects of the storm tide and astronomical tide from scientific and anecdotal documents. Tide gauge data were unavailable during surge periods, or gauges were not located in the area of peak storm surge, so in many cases, the removal of astronomical tidal influences was not possible. Generally, these estimations provided water levels slightly above normal, sometimes rounded off to the nearest foot, which were then converted to meters.

The rest of the 10 records have been compiled from Murty et al. (1986), Khalil (1992), and Murty and El-Sabh (1992). The reported surge was given with a qualitative location similar to the SMRC. The same approach was used to quantify these locations.

Figure 3.1 shows the locations of peak storm surges with grayscale gradient symbols showing various scales of surge intensity. Four of the storm surges (1974, 1975, 1978, and 1982) are actually recorded over water but are close to land and are considered.

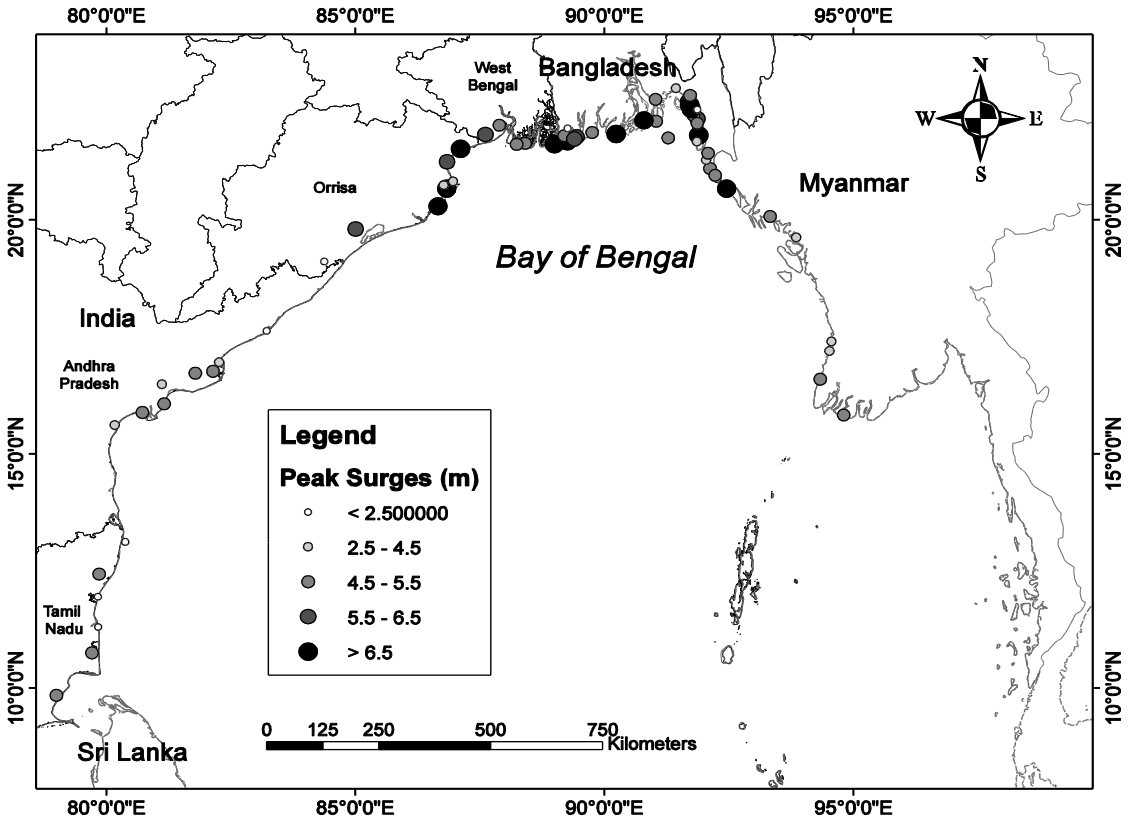

Figure 3.1 − Coastlines of the Bay of Bengal and location of major storm surges in various intensity from 1885–2011

Among the 11 >6.5 m surges, 8 surges occurred on the coast of Bangladesh and 3 on the Indian coast (Orissa). Among the 5.51−6.5 m surges, 4 occurred on the coast of Bangladesh and 3 were on the coast of India (2 and 1 occurred in Orissa and West Bengal respectively). The 4.51–5.5 m surges occurred more frequently than the other categories, where 11 occurred on the coast of Bangladesh, 10 were on the Indian coast (3, 4, and 3

occurred in West Bengal, Andhra Pradesh, and Tamil Nadu respectively), and 4 were on the Myanmar coast. Among the 2.5–4.5 m surges, 4 occurred on the coast of Bangladesh, 5 were in India (2 and 3 occurred in Orissa and Andhra Pradesh respectively) and 3 in Myanmar. There were only 9 surges <2.5 m, where 4 occurred in Bangladesh and 5 are in India (1, 1, and 3 occurred in Orissa, Andhra Pradesh, and Tamil Nadu respectively).

3.1.2 Wind Speed

To best represent and model the relationship between storm surge and wind speed, it is necessary to find the pairing of wind and surge with the strongest statistical relationship. Multiple locations of wind are considered: the reported peak wind at landfall, and the 6-, 12-, 18-, and 24-hour winds prior to landfall.

Latitudinal and longitudinal specification for both surge height and wind provide the level of dependency between wind and surge to analyze risk. For the reported maximum wind, this research utilizes wind speed data from the SMRC and IBTrACS. The SMRC provided 32 wind events for this study from 1949–1997. These events do not come with information regarding where the peak wind was recorded, only where landfall was recorded. Since it is known that peak winds often occur prior to landfall due to the decay influence of the land (Kaplan and DeMaria 2001), assuming that the reported peak wind occurred at the landfall location is not suitable. This is the reason for use of two datasets. DS1 does not include location information for the reported peak wind. DS2, described below, has this information, which may prove useful in the model. The IBTrACS dataset provided an additional 22 wind events from 1885–2011. The rest of the 10 records have been aggregated from renowned journals and publications (Murty et al. 1986, Khalil 1992, Murty and El-Sabh 1992). These winds with the surge described above comprise DS1.

For winds prior to landfall, the tracks of the cyclones with storm surge information have been identified from the IBTrACS using the following few steps. The IBTrACS dataset provided all wind speeds along the cyclone track from 1885–2011. IBTrACS is the most commonly used TC data source and records location, distribution, frequency, and intensity of TCs worldwide. Among the various data sources in IBTrACS, wind speed data have been obtained primarily from the National Center for Atmospheric Research (NCAR): North Indian Ocean Basin: BoB and Arabian Sea, and World Meteorological Organization (WMO) depending on availability. If they were not available in those two sources then the wind data were obtained from different weather observatory stations in IBTrACS. For example, some wind speeds were taken from the IMD: RSMC New Delhi, JTWC, and the National Climate Data Center (NCDC). In IBTrACS, the wind speeds are recorded in knots and have been converted to m s^{-1}. All the cyclone track positions and wind values have been cross-verified with the Unisys Weather (National Weather Service, NOAA) (Unisys Corporation 2015) database.

IBTrACS provides 6-hour intervals of observation for each storm's location and intensity from the time of its formation to its final decay. In this study, according to the National Hurricane Center (NHC), landfall is defined as the location where the TC center intersects with a coastline (NHC 2015). When using the 6-hour track, it is possible to miss the landfall location. The 6-hour track could be just before or just after landfall. The point of landfall for each storm track was identified using a land mask of the study area and the approaches outlined in Needham and Keim (2014). This point was marked as hour zero. A spline interpolation method (Jagger and Elsner 2006) was used on the 6-hourly cyclone track data to capture the hourly values. This provides a clearer picture of landfall location.

Then the interpolated values were used to identify the one-hour geographic position of the cyclone center and wind speed to consider hours 6, 12, 18, and 24 prior to landfall. The various magnitudes of wind speed are used to test the relationship between wind and storm surge at differing points along the cyclones' tracks. The wind speed chosen for final analysis was the variable that produced the strongest significant statistical correlation with surge and is used in DS2. These correlations will be discussed below.

Among the 64 events, five storms (1952, 1960, 1963, 1970, and 1971,) did not make a landfall as defined by NHC. However, these tracks passed close to land and have peak surge records worth modeling. Hour zero was marked as the track point closest to the land mask. Among these nine cyclone tracks the closest track is about 0.45 km from the coastline, the farthest is about 277 km from the coastline, and the average distance from the decay point of the track to the coastline is about 94 km. The distances measured in these cases considered the nearest coastline from the decay point. For each track considered in this study, the average track length from cyclogenesis to total decay is 1853.22 km. Figure 3.2 shows the cyclone intensity scale with color gradient lines followed by the IMD.

3.1.3 Combined Wind and Storm Surge Datasets

Using the data outlined above, 64 storm surge records with maximum winds occurred along the coast of the BoB from 1885−2011. No storm events are included outside of these ranges due to a lack of observational surge data. The data set includes the name, country of landfall, year of the cyclone, surge height in meters (SmaxM), longitude (Slon) and latitude (Slat) of the surge height, recorded peak wind in m s^{-1} (MaxW), wind speed at 6(6W), 12(12W), 18(18W), and 24(24W) hours prior to landfall, longitude (MWlon) and latitude (MWlat) of the peak wind, longitude (12Wlon) and latitude (12Wlat) of the

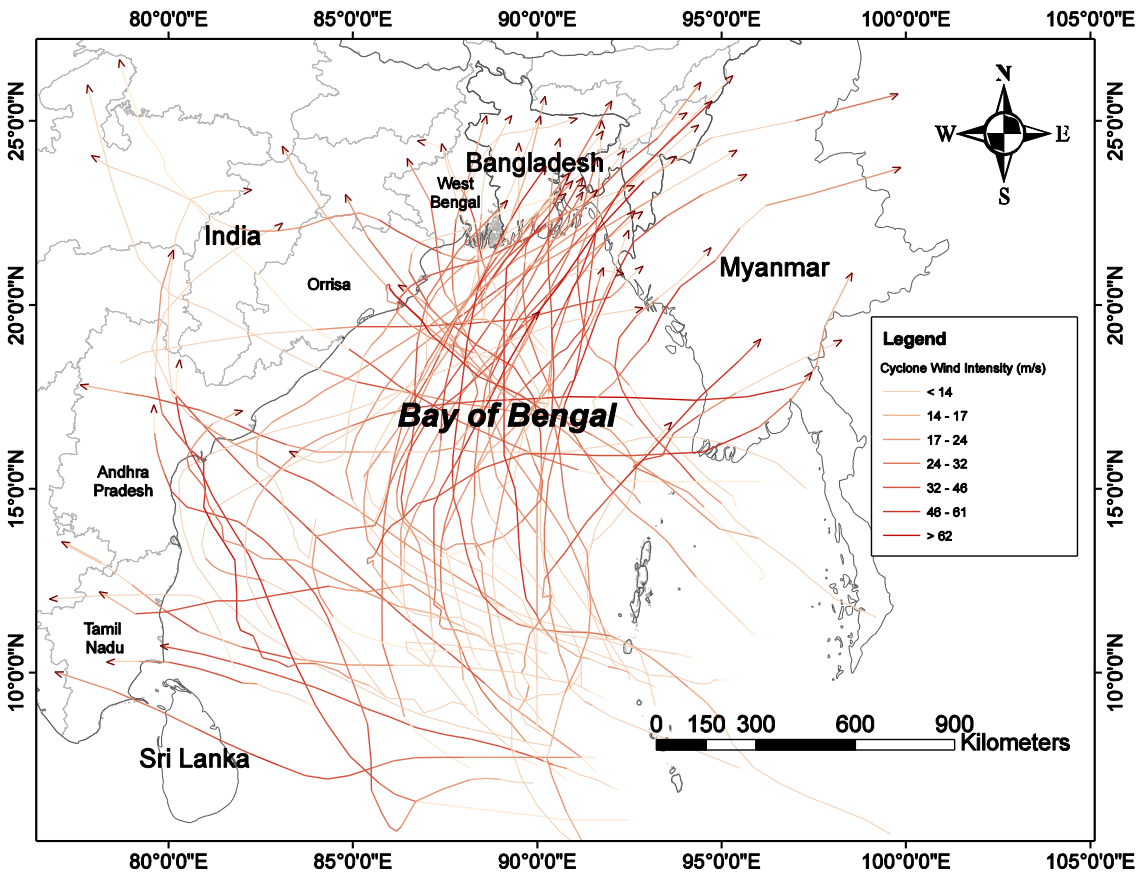

Figure 3.2 − Along-track wind intensity of the Bay of Bengal storms, 1885–2011. The category of wind intensity follows the IMD classification

wind speed 12 hours prior to landfall, and the distance between 12W and surge in meters 12 hours before landfall (D12) (see Appendix). An index is added to the data that notes the position of the cyclone wind along the track relative to the surge location. This is only applicable to the 12W in DS2 as the wind is on the cyclone track. If the wind speed occurred to the left of the surge location, it was given an index of 1. If the wind speed occurred to the right of the surge location, it was given an index of 0. It is well-known that the highest magnitude of wind speeds is in the right front quadrant in the Northern Hemisphere, (NOAA 2015). This index is used in later regression analyses as an attempt to test that relationship.

Among the 64 storm surge records with maximum winds, there is only one storm surge event in the 1800s. This event has been reported in multiple documents due to the severity and damage. Frequency of storm surge events is higher during later portions of the record. This is likely due to the establishment of more weather observatory centers at the local and national level and improvement of the technology after the 1950s. When considering any time series analyses or any modeling that involves rate information, this earlier record will be omitted due to the potential data bias.

For the storm surge events that do not have any reported wind speed records, the track of the cyclone has been identified from the IBTrACS data set and maximum wind speed has been traced along the track for that specific event. As mentioned earlier, 22 records for winds have been collected from IBTrACS to pair with 5 SMRC and 17 SURGEDAT surge records that do not come with wind data.

3.2 Relationships between Surge and Wind

In this research, the strongest statistical relationship between wind and storm surge is needed to model the combined risk of both cyclone characteristics. Multiple locations of wind are considered: the reported peak, and the 6-, 12-, 18-, and 24-hour winds prior to landfall (as described above).

Upon initial analysis of the distributions, the storm surge and reported peak winds are normally distributed and pre-landfall winds are non-normally distributed (Figure 3.3). The Shapiro-Wilk test (Royston 1982) is performed to test the normality and cross validate the distributions. From the test, the p-values for storm surge, 12-hour pre-landfall wind and peak wind are respectively 0.15 (> 0.05), 0.005 (< 0.05) and 0.31 (> 0.05). Higher p-values for storm surge and peak wind show no significance and state the notion that samples are

normally distributed. The lower p-value for 12-hour pre-landfall wind suggests the values do not come from a normal distribution. This makes physical sense as many events have lower magnitude wind speeds and few have extreme wind speeds. Thus, the Pearson product-moment correlation is used for the peak wind and the Spearman's rank correlation is used for the pre-landfall winds to represent the statistical relationship between all surge and wind pairs. A total of 64 records have been considered for correlation analysis and the results can be seen in Table 3.1. The strongest relationships are noted in shaded rows.

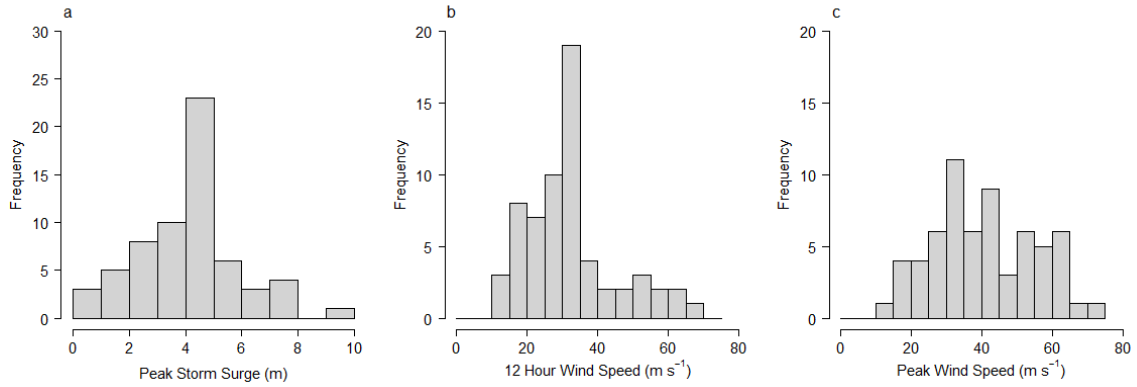

Figure 3.3 − Frequency distribution of (a) surge height (meters), (b) peak wind (m s^{-1}) and (c) 12-hour pre-landfall wind (m s^{-1})

The most significant correlations are found between the reported peak wind and surge height ($r = 0.51$, p-value < 0.00). Because the reported peak winds do not come with latitudinal and longitudinal coordinates, the research must analyze the surge relation with winds before landfall (where location information is known). Previous research shows that pre-landfall winds are correlated more strongly with storm surge height than winds at landfall (Jordan and Clayson 2008; Needham and Keim 2014). Jordan and Clayson (2008) explained that a certain amount of time is required for a water column in an ocean to gain energy from its adjacent atmosphere. For the U. S. Gulf Coast, Needham and Keim (2014)

determined that among pre-landfall winds, winds 18 hours before landfall have a stronger correlation when compared to wind speeds at other pre-landfall hours. In this study, among the pre-landfall winds considered, the strongest relationship to storm surge height is found at 12 hours before landfall ($\rho = 0.3$, p-value = 0.01) (Table 3.1). The amount of variance explained by the Pearson r value is the square of the value. This difference in the 12-hour pre-landfall correlation may be attributed to different geographical settings and dynamic systems (Ali 1979) associated with the cyclone formation in the BoB versus the Gulf of Mexico. The two datasets utilizing the reported peak wind (DS1) and 12-hour pre-landfall winds (DS2) are used for the duration of the analyses presented throughout the remaining chapters of this thesis.

Table 3.1 − Pearson's product moment and Spearman's rank correlation values between cyclone winds and peak surge heights

Categories of Wind with Surge Events	Pearson's		Spearman	
	r	P-value	ρ	P-value
Reported Peak Wind	0.5093569	1.72e-05	0.4829145	5.31e-05
6-hour Pre-landfall Wind	0.3234496	0.009132	0.25652	0.04075
12-hour Pre-landfall Wind	0.3503721	0.004535	0.3142554	0.01144
18-hour Pre-landfall Wind	0.3409144	0.005839	0.3098499	0.01272
24-hour Pre-landfall Wind	0.2691565	0.0315	0.2413131	0.05474

CHAPTER 4.
METHODS AND RESULTS

All analysis and modeling is performed using the open source software, R Project for Statistical Computing (R Core Team 2014). Specifically, the **copula** package (Yan 2007; Kojadinovic and Yan 2010) is utilized for the final portion of analysis of the research. Copula is a combined risk analysis package built under R environment. Before creating the copula model for DS1 and DS2, basic descriptive statistics and regression results are presented.

4.1 Descriptive Statistics

Each dataset has 64 event records. Of those 64, 56% were recorded at the coast of Bangladesh, 36% occurred along the east coast of India, and 8% were on the coast of Myanmar. When considering the entirety of the surge data, the Myanmar coast was affected by the highest surges in 1982 (Cyclone Gwa) and 2008 (Cyclone Nargis). These cyclones caused extensive loss of life and property along the Myanmar coast and farther inland (Dube et al. 2009). The east coast of India has received devastating storm surges in 1971, 1977, 1989, 1990, 1996, and 1999 (SURGEDAT 2015) in terms of surge height. Along the east coast of India, the Andhra Pradesh coast (Figure 1.1) experienced the most events, where 39.1% of TCs included in this record made landfall. The next most frequent location is along the Orissa coast and Tamil Nadu coast where 26.1% of TCs made landfall. A total of only 8.7% of TCs crossed the West Bengal coast.

For the Bangladesh coastline, locations of the storm surges show that the Noakhali-Chittagong coast and Barisal/Patuakhali-Noakhali coast are much more susceptible to storm surges than other areas, with the maximum storm surge height in the sample considered here being 10 m (the Bhola Cyclone). The Chittagong-Cox' Bazar coast is a

secondary peak area of susceptibility, with a maximum storm surge height of 7.6 m (Barisal-Bakerganj Cyclone). The Khulna/Sundarban and Barisal-Noakhali coasts are relatively less vulnerable in comparison to the above-mentioned locations.

The minimum surge height recorded from 1885–2011 (Table 4.1) was 0.2 m (Chennai Cyclone in 1978) and the maximum surge recorded was 10 m (the Bhola Cyclone in 1970), with an average 4.6 m surge height over the years. The average peak wind speed and 12-hour pre-landfall wind speeds were 40.66 m s^{-1} and 32.6 m s^{-1}, respectively. The minimum storm surge, peak wind and 12-hour pre-landfall wind speed occurred during the same event in 1978, with 0.2 m, 10.29 m s^{-1}, and 10.35 m s^{-1}, respectively. The maximum peak and 12-hour pre-landfall wind speeds were 72.02 m s^{-1} and 68.84 m s^{-1}, respectively, and occurred in 1999 when the surge height was 7.5 m.

Table 4.1 − Summary of variables. Min is the minimum, Max is the maximum, 1Q and 3Q refer to the first and third quantiles

Surge (m)	Peak Wind (m s^{-1})	12-hour Pre-landfall Wind (m s^{-1})
Min: 0.200	Min: 10.29	Min: 10.35
1Q: 3.375	1Q: 30.42	1Q: 23.46
Median: 4.550	Median: 38.60	Median: 31.86
Mean: 4.299	Mean: 40.66	Mean: 32.16
3Q: 5.000	3Q: 53.61	3Q: 35.16
Max: 10.000	Max: 72.02	Max: 68.84

The monthly distribution of cyclones included in this record is shown in Figure 4.1. Cyclones occurring in this region show bimodal peaks: one in May, and the other in October. May is the most susceptible month, with 28.6% of BoB TCs included in this record making landfall somewhere in the basin. Specifically along the eastern coast of India, 30.4% and 34.8% of TCs make landfall in October and November, respectively. For the Bangladeshi coast, May and October are the most susceptible months with 30.6% and 25% making landfall, respectively.

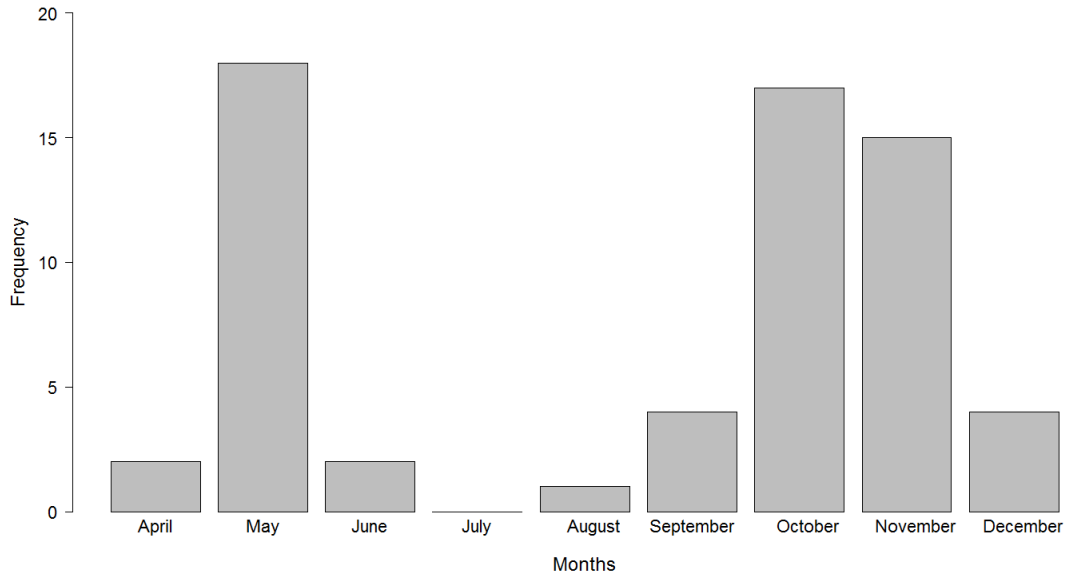

Figure 4.1 − Monthly frequency distribution of cyclones occurring in the Bay of Bengal from 1942-2011

4.2 Regression Analyses

Regression analysis is a statistical process to examine relationships between a variable of interest and explanatory variables. The regression equation is written as $y_i = \alpha + \beta x_i + \varepsilon_i$, where y is the dependent variable, α is the intercept, β is the slope of the line, *x* is the independent variable, and ε is the error term. Here, different regression models are presented. First, as an attempt to look at trends over time, time series analyses are presented to quantify relationships between year and storm surge height and year and the two wind speed variables.

The intensity of peak storm surge height, peak wind, and the 12-hour pre-landfall wind as a function of year are shown in Figure 4.2(a–c). To avoid potential bias in the time record, the 1885 event has been removed from each dataset for the rest of the analyses and the new start date of the data is 1942.

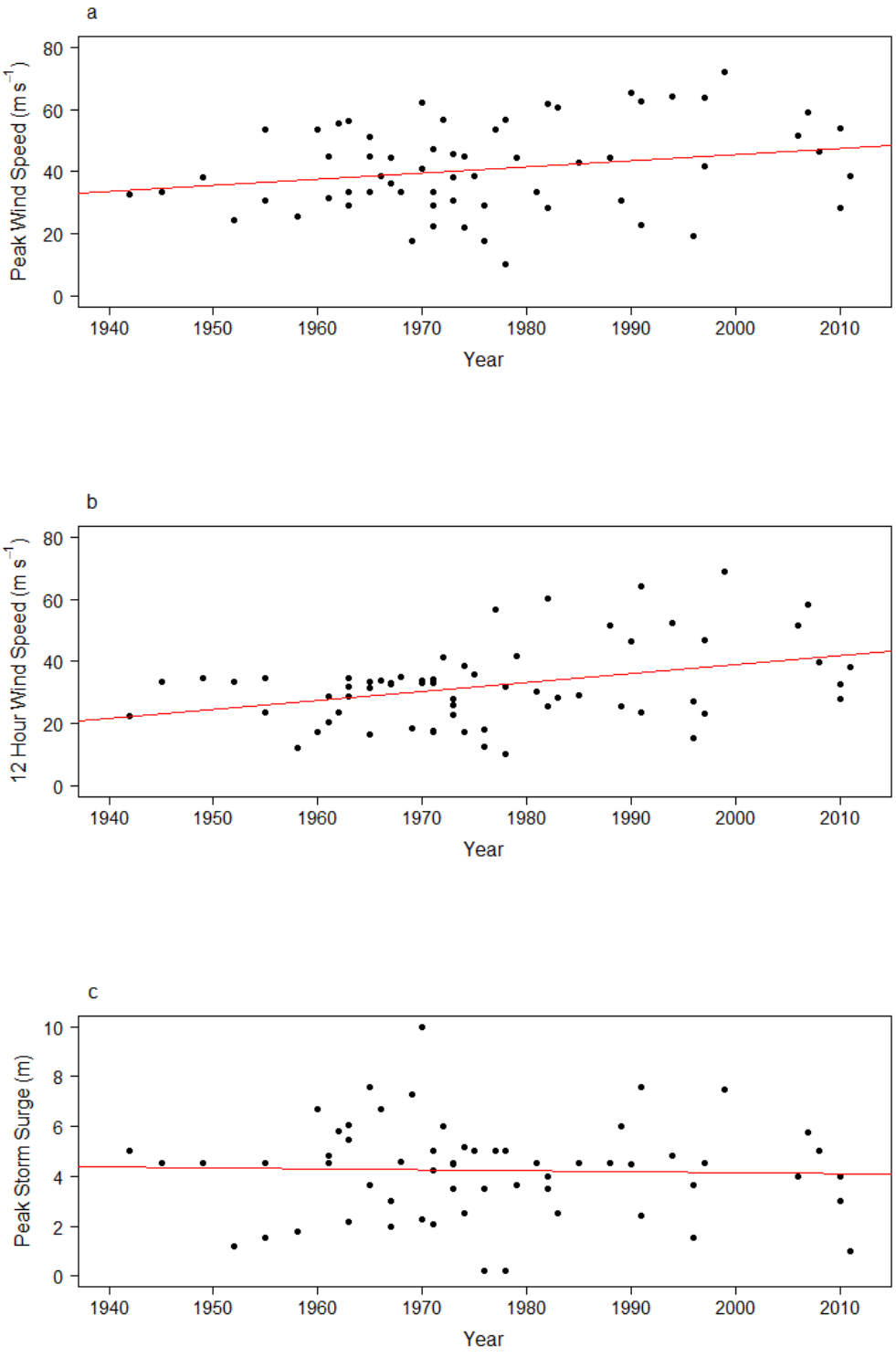

Figure 4.2 − Scatterplots between (a) year and peak wind, (b) year and 12-hour pre-landfall wind, and (c) year and storm surge

The time series models in Figure 4.2(a) and 4.2(b) show a slightly increasing temporal trend for both for both peak wind speed and 12-hour pre-landfall wind speed. The slope of the Figure 4.2(a) shows for every one year that passes, peak wind speed increases by 0.20 m s^{-1} (p-value = 0.07). The slope in Figure 4.2(b) shows for every one year that passes, the 12-hour pre-landfall wind speed increases by 0.30 m s^{-1} (p-value = 0.002). For both wind sets, the models show at least marginally significant results. It is possible this increasing trend is due to changes in warmer SST (Nitta and Yamada 1989; Cane et al. 1997), or changes in better measurement techniques over time. On the other hand, the linear regression model in Figure 4.2(c) shows a slightly decreasing trend of peak storm surge height over time. The relationship between storm surge and year is not significant (p-value= 0.79), indicating there is not a trend across time in storm surge values for the BoB.

Storm surge height can be described with wind values by using a regression model. Initially, a Pearson product-moment correlation was computed to find relationships between peak surge and various levels of winds using all data back to 1885. This was presented in Chapter 3 as a way to describe the choice of wind speed data for analysis. Again, to avoid the concern over the potentially missing events in the first portion of the 20th century, 1942 is the new start date. Correlation values between the new DS1 and DS2 variables are minimally different and still significant. For peak wind, the Pearson correlation value is 0.512 (p-value < 0.0000). The Spearman rank correlation value for the 12-hour pre-landfall wind data is 0.345 (p-value = 0.0057). Both tests show the correlation is strong for peak wind with a highly significant p-value, and moderately strong for the 12-hour pre-landfall wind with a less significant p-value. The assumptions of a linear model are that the data are normally distributed and the data values are independent and identically

distributed. These assumptions are tested through analysis of the regression model residuals.

The peak reported wind data are normally distributed and can be modeled using linear regression without breaking any assumption rules. On the other hand, the 12-hour pre-landfall wind data show positive skewness for the distribution. In this case, the residuals of the regression model are analyzed to assess the fit of the model and to validate use of a linear regression with slightly skewed data.

An ordinary-least squares (OLS) regression model was created for peak winds and the 12-hour pre-landfall winds. As a first order, the R program package **ggplot2** (Wickham 2010, Wilkinson 2011) has been used for each storm and wind pair to visualize the relationship.

Figure 4.3(a) shows the relationship between the reported maximum wind speed (m s^{-1}) and surge height (m), and Figure 4.3(b) shows the relationship between the 12-hour pre-landfall wind speed (m s^{-1}) and surge height (m). The marginal distributions of winds and surge are also shown along the x and y axes. The red line indicates the best fit model.

Figures 4.3(a) and 4.3(b) show significant trends between wind speeds and surge height. The significant (p-value <0.000) relationship between peak wind and surge height shows that for every 1 m s^{-1} increase in wind speed, surge heights are expected to increase by 0.07 m. Also, for every 1 m s^{-1} increase in 12-hour pre-landfall wind speed, the storm surge significantly (p-value = 0.001) increases by 0.05 m. However, storms with higher wind speeds do not always cause the higher surge. Storms with higher wind speeds do not always have the higher surge.

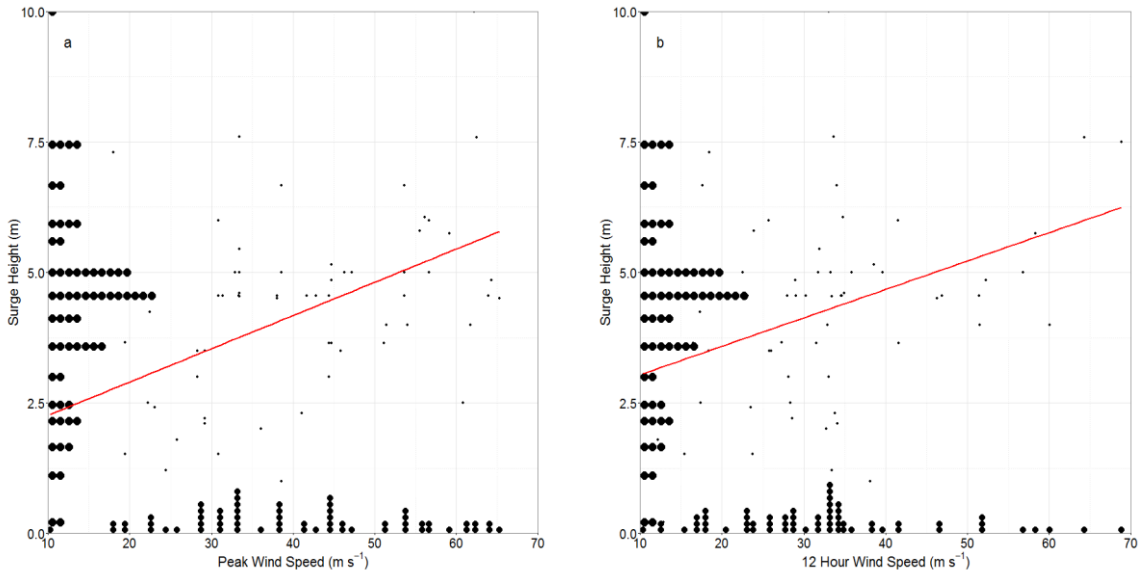

Figure 4.3 – (a) Peak wind speed (m s^{-1}) and (b) 12-hour pre-landfall wind speed regressed on storm surge height (m) at the Bay of Bengal. The adjacent axes show the marginal distributions of the respective variables

To assess whether assumptions were violated in the peak and in the 12-hour pre-landfall wind speed and storm surge regression models, residuals are analyzed from the model fit. Figures 4.4(a) and 4.4(b) show the distribution of residuals of the regression model of peak wind and 12-hour pre-landfall wind, respectively. Both histograms are similar to a normal distribution. P-value from the Shapiro-Wilk test (Royston 1982) is 0.053 for the residuals in peak wind and surge model and 0.27 for 12-hour pre-landfall wind and surge model respectively show that the distribution is marginally significant and not significant. In both cases it support the notion that the residuals are normally distributed. This offers no reasons to reject the validity of the linear regression model of both datasets.

The relationship between wind and surge is modeled sequentially including a third variable: position of the wind speed relative to the surge and then distance between surge and wind location. The modeled relationships are: (i) how does wind affect surge, (ii) how

does wind and distance from wind to surge location affect surge, and (iii) how much influence does the position of the peak wind relative to the surge location have on surge. In the Northern Hemisphere, the peak of a storm surge is generally higher to the right of the cyclone track or cyclone wind direction, as these areas receive strong onshore winds from the counterclockwise wind flow around the cyclone (Needham and Keim, 2014) and over that extensive area water continues to pile up in a pronounced way (Blain et al., 1994). As mentioned previously, if the surge occurred to the right of the wind location, it is given an index of 1 and for the opposite case, a value of 0. In a study by Blain et al. (1994), if a tropical cyclone travels to the left of the surge event, the right front quadrant would be closer to the surge (Trepanier 2012). Since the peak wind and surge height of the SMRC were recorded in the same location, the DS1 data set does not contain any index or distance measurement. For DS2, one hypotheses is that cyclone wind speed occurring to the left of the surge event will produce a higher surge than one occurs to the right. Using a logistic regression the index variable is considered. The relationship is not significant.

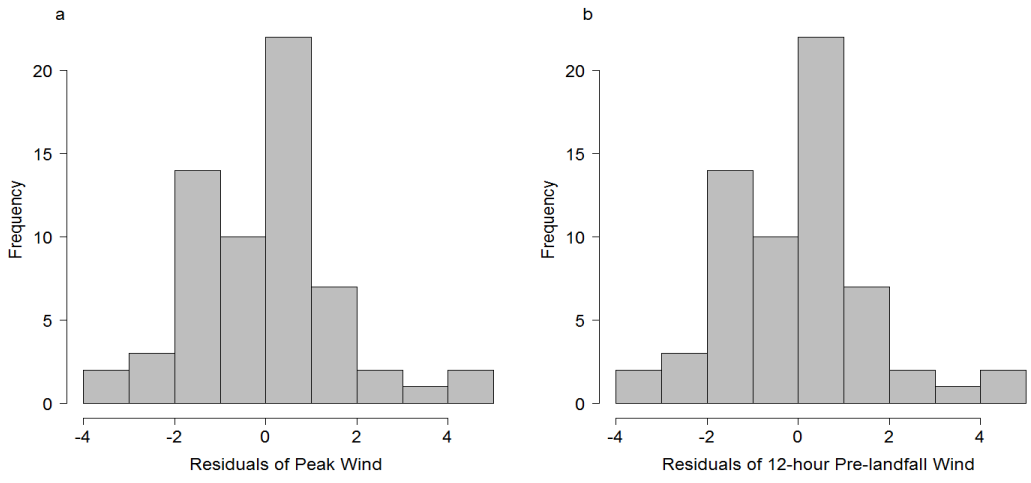

Figure 4.4 − Distribution of residuals (a) of peak wind and (b) 12 hour pre-landfall wind

A distance variable as described above shows a weak correlation value with surge of 0.24 (p-value = 0.06) and leads to a suggestive rejection of the null hypothesis that there is no relationship and the acceptance that the distance between the wind and surge location influences the surge height, at least marginally. The variable is examined further in a regression model. For every 1 m s^{-1} increase in 12-hour pre-landfall wind speed, surge heights are expected to increase by 0.06 m (p-value = 0.001). For every 1 km increase between the wind and surge height locations, surge is expected to increase by 0.004 m (p-value = 0.01). This suggests that the greater the distance between the 12-hour pre-landfall wind and peak surge, the greater the surge tends to be. Distance between the 12-hour pre-landfall wind and peak surge gives the ocean more time and more space to response to changes in the wind speeds. This suggests the model can be improved by including the distance from wind to surge location.

The Akaike Information Criterion (AIC), which is a measure of the goodness of fit of a statistical model, has been applied to test the quality of the models in comparison to each other, and thus select the best model for further analysis. The lower the value, the better the model describes the relationship. The three relationship models described above get the AIC test values of 252.9 (model=i), 249.5 (model=ii), and 254.88 (model=iii) respectively. These values indicate that the model using the 12-hour pre-landfall wind with the distance between the wind and surge location is better than using just the 12-hour pre-landfall wind alone. Therefore, a copula model is presented for both DS1 and DS2. DS1 has the stronger relationship between the peak wind and the storm surge and landfall and is, thus, important to model. DS2 is used to create a copula because this information comes with additional location information. The AIC value suggested that knowing this

information furthers the understanding of the expected surge at landfall. Depending on the application, either data set may be useful.

Copula modeling minimizes the marginal distribution influence and runs the joint distribution of storm surge and wind speed to predict the dual risk at the coast of the BoB. The magnitude of inundation due to surge varies with the tidal conditions and associated landforms. This research is directed toward a broader analysis of storm surge and wind risk, where risk can be defined as statistical likelihood of the storm surges and wind speeds affecting the coast of the BoB.

4.3 Copula Model

To understand the relationship between cyclone wind speed and storm surge and to estimate the overall risk, i.e., the likelihood of a wind and surge occurring in the BoB from cyclones, a bivariate statistical copula is used.

A copula is used to describe the dependency structure between the wind speed (peak wind and 12-hour pre-landfall wind) and peak storm surge height to quantify statistical risk along the BoB coastline. The dependency structure describes the behavior of one random variable given the occurrence of another. That is, a copula model can be used to describe how surge and wind are linked with one another within a TC system. Physically, cyclone wind and storm surge are linked because they share many of the same processes within the TC. The atmosphere-ocean flux which drives the TC storm surge is created through the momentum flux between the energy exchange of the winds near the ocean surface and the waves at the top of the ocean water column (Trepanier et al. 2015). Thus, stronger winds generate a greater flux. It is worth noting that the swell of the water column and amplification of surge near landfall depend on many characteristics including, but not

limited to, the continental shelf and bathymetry; not just on the relationship with wind speed.

The objective of a copula is to model the dependence of wind and surge (*W,* S) statistically. It can be assumed that the marginal distributions of random variables are the same and that the data can be treated as such within the copula model. However, as the marginal distributions of random variables are often not identical, the copula function can be written to allow for the removal of marginal influences. It sets up the goal to predict the annual probability for a given occurrence level of wind speed and storm surge. The dependence measure for wind and surge (*W*, *S*) developed finds a return period (year), *Z*, for a given occurrence level of wind speed and storm surge. Tawn (1988) and Coles et al. (1999) describe the theory and dependence models for extreme values. The theory is summarized below.

The copula function for a measure of dependence in the extreme tail is described as follows. For any random vector, (*W*, *S*), the distribution function F (w, s) = Pr (*W* ≤ w, S ≤ *s*) provides a complete description of dependence between variables *W* and *S.* The effect of the margins are removed by observing that, subject to continuity conditions, there is a unique function C (., .) with domain A = [0,1] × [0,1] such that

$$F\,(\mathrm{w},\,\mathrm{s}) = C\,[F_W(w),\,F_S\,(s)], \qquad (1)$$

where F_W and F_S are the marginal distribution functions given by

$$F_W(w) = F\,(w,\,\infty),\ \text{and}\ F_S\,(s) = F\,(s,\,\infty). \qquad (2)$$

The function *C* is the copula model and it contains the information about the joint distribution of *W* and *S* apart from the marginal distributions. *C* describes the association between the two variables after transformation to variables *U* and *V*, having margins

defined by the empirical data distributions. Analysis of the data distributions allows a distribution to be chosen for the margins and the attention can then be focused on the dependence structure between surge height and wind speed. Joe (1997), Nelsen (1998), Coles et al. (1999), and Yan (2007) give a complete summary of the dependence measures. In this thesis, a two-dimensional copula model has been implemented based on the sample values. The dimension is the number of variables, in this case wind and surge.

4.3.1 Elliptical and Archimedean Copula Structures

The dependency structure of wind and surge can be modeled with various classes of a copula. In this study, two important classes considered are the elliptical and the Archimedean copula families and each are applied for combined risk modeling of wind and surge. The model with the best fit provides a table of annual probabilities of specific wind and surge pairs with uncertainty provided with 1000 Monte Carlo simulations of the copula.

First, the structure of elliptical copulas are described followed by a description of the Archimedean copula. Elliptical copulas are simply the distribution functions of componentwise transformed elliptically distributed random vectors. The model is derived from multivariate distribution functions using Sklar's Theorem (Fang et al. 1990, Embrechts et al. 2001). Elliptical distributions, which are comparably rich in parameters, enable the modeling of multivariate extremes by sharing tractable properties of the multivariate normal distribution (Embrechts et al. 2001). Let F be the multivariate cumulative density function (CDF) of an elliptical distribution, F_i is the CDF of the i^{th} margin, and F_i^{-1} is its inverse function, i = 1, . . . , p. The elliptical copula determined by F is

$$C(u_i, \ldots, u_p) = F\,[F_1^{-1}(u_1), \ldots, F_p^{-1}(u_p)] \qquad (3)$$

In this family are two common elliptical copulas: the Gaussian (or normal) and the Student's t. The Gaussian copula has been implemented in this study for the two-dimensional bivariate case of wind and surge for both data sets (DS1 and DS2). The bivariate distribution function for the Gaussian copula is parameterized by the linear correlation coefficient ρ and is expressed as:

$$C(u, v) = \Phi\rho\,(\Phi_\rho^{-1}(u), \Phi_\rho^{-1}(v)) \qquad (4)$$

where $\Phi\rho(\cdot, \cdot)$ is the bivariate Gaussian distribution function and $\Phi-\rho\,1(\cdot)$ is the inverse of the univariate Gaussian distribution function (Louie 2014). The model was also tested using a copula created with a t-distribution. Little difference was found in the results.

Archimedean copulas are an important class of copulas that have closed form expressions and allow for a great variety of different dependence structures (Embrechts 2001). They are able to capture different kinds of tail dependencies, such as: only upper tail dependence and no lower tail dependence or both lower and upper tail dependence but of different magnitude (Hofert and Mächler 2011). This class of copulas are very popular and advantageous for some settings as the relationship can be expressed in terms of a single-argument generator function $\varphi(t)$ (Embrechts et al. 2001, Nelsen 2007; Nelsen et al. 2002) rather than C(u, v), (Louie 2014). The expression can be written as,

$$C(u_1, \ldots, u_p) = \varphi^{-1}\,\{\varphi(u_1) + \cdots + \varphi(u_p)\} \qquad (5)$$

where φ^{-1} is the inverse of the generator ϕ. While this multidimensional definition formally follows the criteria of a copula under certain properties of φ, higher dimensions are not practical since the margins are exchangeable. Therefore Archimedean copulas are mostly used in the bivariate case (Schölzel and Friederichs 2008). Commonly used examples of

Archimedean copulas include the Clayton (Clayton 1978), Frank (Frank 1979), and Gumbel (Gumbel 1960). All these three families of Archimedean copula have been tested for DS1 and DS2 and it has been found that the Gumbel copula fits both data sets well. The Gumbel copula is an extreme value copula which allows us to model tail behavior of joint distribution and focuses on upper tail. The Gumbel copula has been used in this study for two dimensional bivariate case of wind and surge to model their tail dependencies for both DS1 and DS2. The generator function which is related to a bivariate copula is:

$$C(u, v) = \varphi^{-1}(\varphi(u) + \varphi(v)) \qquad (6)$$

where $\varphi^{-1}(\cdot)$ is the pseudo-inverse of $\varphi(t)$. For the Gumbel copula the generator, $\varphi(t) = (-\ln t)\,\alpha$ and generator inverse, $\varphi^{-1}(s) = \exp(-s^{1/\alpha})$.

Although simulation from elliptical copula is straightforward, there are drawbacks in elliptical copulas as they are restricted to have radial symmetry ($C = \hat{C}$) and do not necessarily exist in closed form expressions (Embrechts et al. 2001, Schölzel and Friederichs 2008). Often many practical applications require different upper and lower tail behavior, which cannot be modeled with an elliptical copula. Such asymmetries can only be explained with Archimedean copulas. Archimedean copula allows a margin to be defined by an extreme value.

4.3.2 Copula Structure for Peak Winds (DS1)

Both elliptical and Archimedean copula model structures are applied to DS1. Using the elliptical copula model structure, the wind and surge data are fitted to normal distributions. Using the Archimedean structure, the wind data are fitted to a Weibull distribution and a normal distribution is used for surge. These decisions were made after attempting to fit to various distributions, including but not limited to the gamma, log-

normal, t, and Poisson. The normal and Weibull created the best fit copula, as described below. For the normal distributions, the parameters are the means and standard deviations and for the Weibull distribution the parameters are shape (ξ) and scale (σ). The values of the parameters are obtained for the marginals using a maximum-likelihood procedure (Venables and Ripley 2002). The multivariate density is generated from the copula definition and the Gaussian parameters (means and standard deviations) for the elliptical copula and the Weibull parameters (ξ and σ) for the Archimedean copula. For both copula models, the copula-based multivariate density is fitted to the data set using a maximum-likelihood procedure.

The first argument is the data (as a matrix), the second is a multivariate copula with normal or Weibull margins, and the third is a vector containing the original parameter estimates. The copulas are redefined using the modeled correlation parameter values. The multivariate density is generated from the new copula definition and the updated Gaussian and Weibull parameter values. This provides fitted copula models using the observational data in DS1. The densities for both the elliptical and the Archimedean copulas are plotted on a two-dimensional grid spanned by the range of wind and surge values.

Figures 4.5(a) and 4.5(b) show the joint density plot from elliptical and Archimedean copula for DS1. The density plot includes the observed data points. Contours, in units of events per bin size, are plotted at intervals of .001 starting at .001. The bin size is in units of meters times m s^{-1} and the number of bins is 50 times 50 over a range from 0 to 9 m and 5 to 80 m s−1. The match between the model and data appears to be good although the highest surge does not correspond with the fastest wind nor does the fastest wind correspond with the highest surge for a few events. Among the joint density

plots of elliptical and Archimedean copula, it is well illustrated that Archimedean copula model fits better to the distribution of the observed points (Figure 4.5, b). The Archimedean copula density structure is used to calculate the return period probabilities for combined wind and surge pairs.

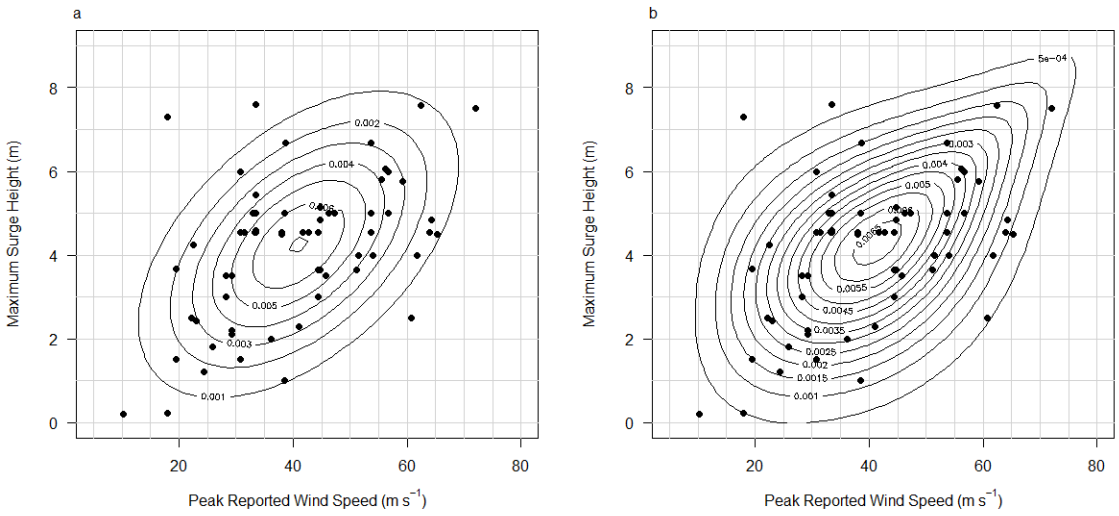

Figure 4.5 − The joint density plot from (a) elliptical copula and (b) Archimedean copula for DS1. The points shown are the empirical data. Peak reported wind speeds (m s^{-1}) are shown on the x-axis and maximum surge heights (m) are shown on the y-axis

The joint probability of the wind and surge based on the copula density is determined using a function created in the R program (R Core Team 2014). The per event probability, [Pr(W > w_{max}, S > s_{max})] times the cyclone frequency (the number of cyclones divided by the total number of years), provides the annual event frequency. That is, the yearly frequency of events with W exceeding w_{max} and S exceeding s_{max}. The yearly probability of an event is then 1−exp(−frequency), where exp() is the exponent function, and the return period is 1 divided by 1 −exp(−frequency), or roughly 1 divided by the frequency plus 0.5 year. For small frequencies, the return period is roughly 1 divided by the frequency. This provides the probability of specific wind and surge events.

Figure 4.6 shows the return period probability of specific wind and surge events using the DS1 data and the copula structure defined above. The lines represent specific years. Contours are given at 2, 5, 10, 20, 30, 50, 75, 100, 150, 200, 300, and 500 years. A 500-year return period has an annual probability of 1/500 or 0.2%.

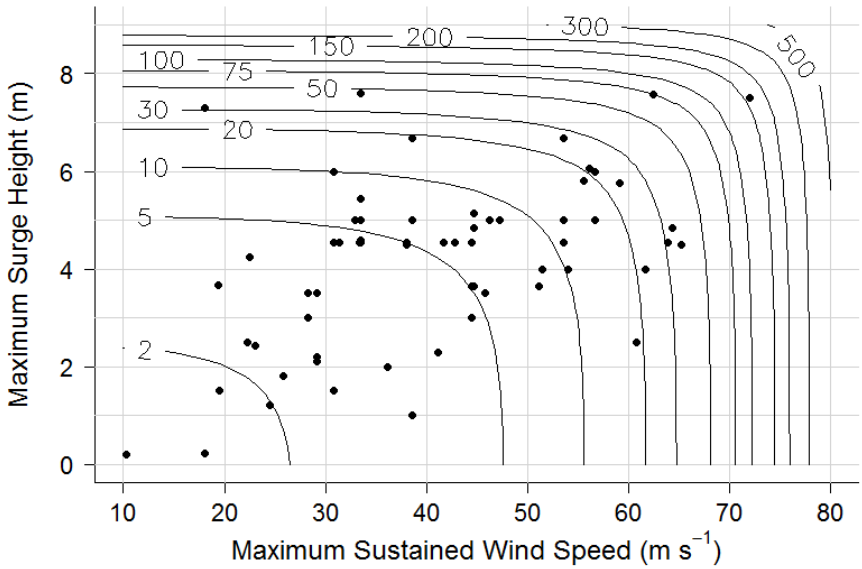

Figure 4.6 − Return period information for wind and surge levels from Archimedean copula for DS1. Each line represents a specific return period year. The years shown are 2, 5, 10, 20, 30, 50, 75, 100, 150, 200, 300, and 500

The combined risk for specific wind and surge pairs have been estimated using the Archimedean copula structure defined above. This is presented in Table 4.2. The classifications of the IMD's cyclone category wind speeds have been followed for this table. Estimates of uncertainty around these point estimates, shown in parentheses, are based on 1000 Monte Carlo simulations. The Monte Carlo simulations use random draws of the normal and Weibull parameters for the marginals (two parameters for the surge marginal and two for the wind marginal, respectively) and a random draw from the copula dependency to generate return periods. The uncertainty is expressed as the 90th percentile of the simulated return periods.

Table 4.2 −Wind speed and surge level return periods for DS1 (from Gumbel copula). Return period year information for (1-4)* cyclone category wind speeds are shown along with 4, 5, 6, and 8 m surges. The quartile pointwise CI is shown in parentheses

Wind Speed (m s^{-1})	Return Period (Year) with 90% Confidence Intervals			
	Surge Height (m)			
	4	5	6	8
24	3.2 (2.7–3.8)	5.1 (4.2–6.9)	10.5 (7.6–17.4)	79.7 (38.8–240.8)
32	3.6 (3.0–4.4)	5.6 (4.5–7.8)	11.1 (7.9–18.3)	81.2 (39.5–251.1)
46	6.0 (4.7–8.3)	8.2 (6.3–12.7)	14.2 (9.9–26.1)	87.9 (42.9–284.1)
62	22.5 (13.8–48.2)	25.7 (15.6–58.5)	33.1 (19.8–81.0)	115.4 (55.8–381.1)

* 1 = Severe Cyclonic Storm, 2 = Very Severe Cyclonic Storm, 3 = Extremely Severe Cyclonic Storm, 4 = Super Cyclonic Storm

Statistical significance exists between pairs that do not have overlapping confidence bounds. For example, on average, the BoB can expect a TC with a peak wind speed of at least a 24 m s^{-1} *with* a 4 m surge every 3.2 years (2.7–3.8). The same peak wind speed with a higher storm surge of 5 m can be expected, on average, every 5.1 years (4.2–6.9). These two events have a statistically significant difference in their recurrence time based on the narrow, non-overlapping confidence intervals. The most extreme event with a peak wind of 62 m s^{-1} and an 8 m surge can be expected to happen once every 115 years.

4.3.3 Copula Structure for 12-hour Pre-landfall Winds (DS2)

Like DS1 both elliptical and Archimedean copula model structures are applied to DS2. Using the elliptical structure, the wind and surge data are fitted to normal distributions and, using the Archimedean structure, the wind and surge data are fitted individually to Weibull distribution for wind and normal distribution for surge. The setup for these different copula structures is exactly the same as described for the peak wind, only using the 12-hour wind data in DS2. This provides fitted copula models for DS2.

Figures 4.7(a) and 4.7(b) show the joint density plot from the elliptical and Archimedean copulas for DS2. The density plot includes the observed data points. Contours, in units of events per bin size, are plotted at intervals of .001 starting at .001. The bin size is in units of meters times m s^{-1} and the number of bins is 50 times 50 over a range from 0 to 9 m and 5 to 80 m s^{-1}. Among the joint density plots of elliptical and Archimedean copula, it is well illustrated, again, that the Archimedean copula model fits better to the distribution. From this point, the Archimedean copula is used to calculate the return periods for wind and surge.

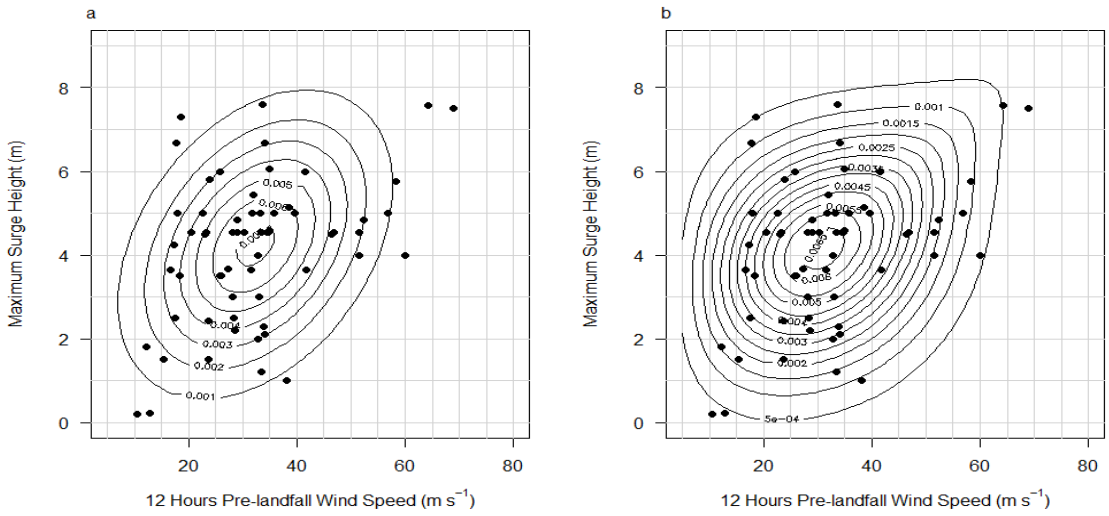

Figure 4.7 − The joint density plot from (a) elliptical copula and (b) Archimedean copula for DS2. The points shown are the empirical data. 12-hours pre-landfall wind speeds (m s^{-1}) are shown on the x-axis and maximum surge heights (m) are shown on the y-axis

From the joint density plot it appears that higher wind speeds do not always cause the higher surges, just like with the peak wind data. This may be due to land water orientation, tidal condition during surge, intensity of a storm, its size, translational speed, angle of approach to the coast, landfall location, or the bathymetry at that location. These uncertainties at the upper tail are explained well by the Gumbel copula of Archimedian

class as it fits the data comparatively well when compared to the elliptical copula and thus is the most appropriate for the combined risk analysis. In Figure 4.8, the return period probability of specific wind and surge events are shown for DS2. The lines represent specific years. Contours are given at 2, 5, 10, 20, 30, 50, 75, 100, 150, 200, 300, and 500 years.

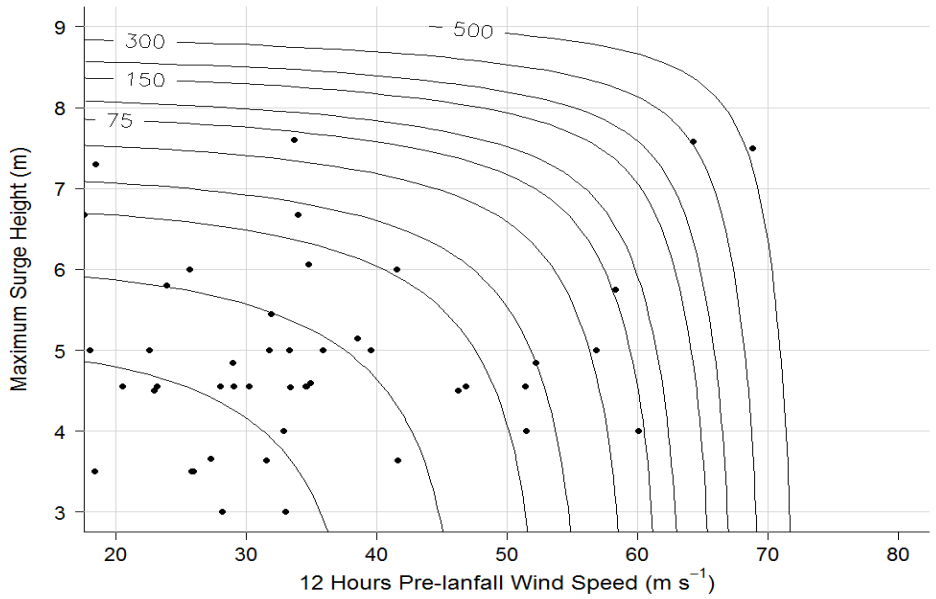

Figure 4.8 − Return period information for wind and surge levels from Archimedean copula for DS2. Each line represents a specific return period year. The years shown are 2, 5, 10, 20, 30, 50, 75, 100, 150, 200, 300, and 500

The combined risk for specific wind and surge pairs have been estimated using the Archimedean copula structure defined above; results are presented in Table 4.3. The classifications of the IMD's cyclone category wind speeds have been followed for this table, as well. Estimates of uncertainty around these point estimates, shown in parentheses, are based on 1000 Monte Carlo simulations, similar to the peak wind copula. The uncertainty is expressed as the 90th percentile of the simulated return periods.

Table 4.3−Wind speed and surge level return periods for DS2 (from Gumbel copula). Return period year information for (1-4)* cyclone category wind speeds are shown along with 4, 5, 6, and 8 m surges. The quartile pointwise CI is shown in parentheses

Wind Speed ($m\ s^{-1}$)	Return Period (Year) with 90% Confidence Intervals			
	Surge Height (m)			
	4	5	6	8
24	3.9 (3.3–4.8)	6.5 (5.1– 9.1)	12.7 (9.0–21.4)	94.8 (44.2–294.8)
32	5.2 (4.2–6.8)	8.2 (6.1–12.1)	15.1 (10.3–26.5)	104.2 (48.8–335.5)
46	12.6 (8.9–21.3)	17.6 (11.5–34.0)	27.6 (16.5–62.8)	139.0 (63.3–541.0)
62	93.5 (40.6–315.4)	109.8 (48.0–397.2)	134.8 (57.0–558.1)	311.8 (117.1–1739.8)

* 1 = Severe Cyclonic Storm, 2 = Very Severe Cyclonic Storm, 3 = Extremely Severe Cyclonic Storm, 4 = Super Cyclonic Storm

Statistical significance exists between some pairs that do not have overlapping confidence bounds. Less significance exists in this table than in Table 4.2. This is potentially due to the stronger relationship between peak wind and storm surge. For example, on average, the BoB can expect a TC with a 12-hour pre-landfall wind speed of at least a 24 $m\ s^{-1}$ with a 5 m surge every 6.5 years (5.1–9.1 years). The same wind speed with a higher storm surge of 6 m can be expected, on average, every 12.7 years (9.0–21.4 years). These two events do not have a statistically significant difference in their recurrence time because their confidence intervals overlap slightly. Significant differences are indicated by a lack of overlap in confidence intervals. The most extreme event with a 12-hour pre-landfall wind of 62 $m\ s^{-1}$ and an 8 m surge can be expected to happen once every 311.8 years. This difference in values for 12-hour pre-landfall wind compared to the peak wind at the highest level is expected as the 12-hour pre-landfall wind is likely closer to the coast and has already begun to feel the effects of land-decay. This difference also represents a singular snapshot in time, whereas the peak wind has the entire length of the track to

occur. The likelihood of that extreme of an event 12 hours before landfall is less than the peak wind.

4.4 Summary of Combined Risk

Comparisons between Table 4.2 and Table 4.3 shows that more time is expected between the occurrence of certain wind speed and surge pairs using the 12-hour pre-landfall data. The risk is greater when using the peak reported wind. The Gumbel Archimedean copula models surge and peak reported wind with greater significance than the 12-hour pre-landfall wind. In addition, the correlation value is higher between surge and peak reported wind. It is rational to say the values presented in Table 4.2 would be more preferable to emergency managers to take further actions. However, as the 12-hour pre-landfall wind provides specific wind location with corresponding surge height, the values in Table 4.3 can be also used to set the boundary for more caution. From both tables it can be generalized that the higher the surge height and wind value the higher the uncertainty of risk. From these results, it seems that in this ocean basin the risk of combined surge heights and wind speeds (even the lowest) are comparably higher than in other ocean basins where the risk is not as great (Trepanier 2012).

CHAPTER 5.
CONCLUSION

5.1 Concluding Remarks

The geographical setting and population density make coastal regions of the BoB more susceptible to storm surge risk and mark it as one of the most active regions of severe TC occurrences, leading to enormous life loss and property damage. Losses result from high winds and the flooding associated with storm surge and rainfall. Statistical models of these two hazards typically take a univariate approach. Various models have been developed to predict storm surge in this region but none of them quantify statistical risk with empirical data. This study shows how peak reported winds along the track and the 12-hour pre-landfall winds (other pre-landfall winds are considered, but the strongest relationship exists at the 12-hour) with associated storm surge heights are related with a statistical model to estimate risk and uncertainty at this coast.

In this research, data have been collected mainly from SMRC, SURGEDAT, and IBTrACS. The SMRC provided reported peak winds with surge heights, which have been updated for recent years from SURGEDAT and IBTrACS. Location specific wind data for the given study period have been collected and interpolated from IBTrACS for associated surge heights. The data show bimodal characteristics of cyclone occurrence with peaks in May and in October. Time series analysis of the data show relationships between year and storm surge heights, and year and the two wind speed variables. For wind values, small increasing trends of wind speed (0.20 m s^{-1} for peak wind and 0.30 m s^{-1} for 12 hours pre-landfall wind) have been observed with marginally significant results. Storm surge data show no trend over time. Regression models also show the relationship between peak storm surge and wind values. There is a strong correlation (0.512) between

storm surge and peak wind speed and a moderately strong correlation (0.345) between storm surge and 12-hour pre-landfall wind speed. In both cases, p-values are significant.

Two classes of copulas have been implemented to fit the model for storm surge and wind-induced risk analysis at the coastline of the BOB. The Gumbel copula of class Archimedean shows the best fit to the data, and reported peak wind and surge height gives the most significant output. Results show that the BoB can expect a TC with a peak reported wind of at least 24 m s^{-1} and a surge height of at least 4.0 m, on average, once every 3.2 years (2.7–3.8), and with a peak reported wind of 62 m s^{-1} and a surge height of at least 8.0 m, on average, once every 115.4 years (55.8–381.1). According to the IMD damage potential scale, 24 m s^{-1} wind intensity forms a cyclonic storm and causes damages to the coastal properties. On the other hand, 62 m s^{-1} wind intensity forms super cyclonic storms and turns into a catastrophic form and causes extensive damage, sometimes total disruption, to coastal structures, roads, embankments, and agricultural lands. Large scale submerging also occur due to flooding and sea water inundation from surge.

5.2 Broader Impacts, Intellectual Merit, and Future Research

The broad impact of this individual study is the hope that locations around the world that experience these natural weather phenomena will adopt this methodology to better understand their statistical risk of hurricanes. Many locations rely simply on the expectation of certain wind levels when there is another deadly factor they should also be considering. This methodology provides a way to assess the frequency of hurricane wind speeds along with hurricane storm surges at any location where surge and wind speed data are available.

The people of this coastal area face the vicious consequences of cyclones more often than any other coastal community in the world. Among the countries that share an Indian Ocean coastline, Bangladesh faces the most consequences because of the extreme population density along the coast (754 per km^2) (BBS 2011).

This research can strengthen early warning or forecasting systems and improve adaptation and coping strategies, cyclone resilience structure, and mitigation measures. Depending on the storm-surge risk level, governments can take initiatives to build embankments/polders and infrastructures along the coastline sustainable to risk level. With this new information, policymakers can develop coastal land use planning and early warning and evacuation systems more suitable to the damage at that area. Moreover, policymakers or government officials could use the information on storm-surge risk to identify vulnerabilities to improve strategies, forecast systems, policies, etc.

The intellectual merit of this study is to provide an analysis using observed data and a statistical copula model to estimate the statistical risk of TC winds and storm surge along the BoB coastline, an area which has not received scholarly attention in this way. Losses result from high winds and the flooding associated with storm surge and rainfall. Statistical models of these two hazards typically take a univariate approach. Copula models estimate the annual probability of the joint hazard. Copulas can be applied anywhere along the coast where storm hazard information is available. They can be used at fixed points along the coast to produce hazard risk maps. Copulas are not restricted to two dimensions and, thus, the methodology can be extended naturally to include other hazard variables such as inland flooding.

Improvements to the model can be made by including structural uncertainty associated with choosing a specific copula type or additional TC variables such as storm size or fetch. This comprehensive method may open a new door to the climate scientist to integrate climatic phenomena with real life situations. The prediction of climate change and the expected increase of intensity of cyclones make the study of TC wind and storm surge even more pertinent (Elsner et al. 2008).

This study will initiate future research for geographers and others in related fields. Statistical risk of TC wind and storm surge occurrence is considerable in terms of time span. By analyzing the frequency, risk, and uncertainty of occurring cyclones with certain wind speed and surge height, coastal managers and policy makers should prepare accordingly. Attention should be given to build capacity, imply land use management and revise mitigation and adaptation policy to minimize the consequences. The application of the copula model will provide useful insights into those initiatives. In broader aspects, this method will identify the on-going and future threats of TC wind and storm surge impacts on coastal ecosystems, property, and live.

REFERENCES

Abrol, V., 1987: Application of a linear surge model for the evaluation of storm surges along the coastal waters of Kalpakkam, East Coast of India, *Indian Journal of Marine Sciences,* **16**, 1−4.

Akter, N., and K. Tsuboki, 2014: Role of synoptic-scale forcing in cyclogenesis over the Bay of Bengal. *Climate Dynamics,* **43**, 2651−2662, doi:10.1007/s00382-014-2077-9.

Alam, E., and A. E. Collins, 2010: Cyclone disaster vulnerability and response experiences in coastal Bangladesh. *Disasters*, **34**, 4, 931−954, doi:10.1111/j.1467 7717.2010.01176.x.

Ali, A., 1979: Storm surges in the Bay of Bengal and some related problems. Dissertation, University of Reading, England, 227 pp.

Ali, A., 1999: Climate change impacts and adaptation assessment in Bangladesh. *Climate Research*, **12**, 109−116.

Azam, M. H., M. A. Samad, and Mahboob-Ul-Kabir, 2004: Effect of cyclone track and landfall angle on the magnitude of storm surges along the coast of Bangladesh in the northern Bay of Bengal. *Coastal Engineering Journal*, **46**, 269–290, doi:10.1142/S0578563404001051.

Bardossy, A., and J. Li, 2008: Geostatistical interpolation using copulas. *Water Resources Research*, **44**, W07412, doi:10.1029/2007WR006115.

BBS, 2011: Population and Housing Census 2011: Socio-economic and Demographic Report. National Series 4, Bangladesh Bureau of Statistics (BBS), Statistical and Information Division (SID), Ministry of Planning, Government of Bangladesh.

Blain, C., J. Westerink, and R. Lucttich, 1994: The influence of domain size on the response characteristics of a hurricane storm surge model. *Journal of Geophysical Research,* **99**, 467–479.

Breymann, W., A. Dias, and P. Embrechts, 2003: Dependence structures for multivariate high-frequency data in finance. *Quantitative Finance*, **3**, 1−14, doi:10.1080/713666155.

BUET, and BIDS, 1993: Multipurpose Cyclone Shelter Program: Report Prepared for the Planning Commission of Bangladesh. United Nations Development Program/World Bank/Government of Bangladesh project BGD/91/025.

Cane, M. A., A. C. Clement, A. Kaplan, Y. Kushnir, D. Pozdnyakov, R. Seager, S. E. Zebiak, and R. Murtugudde, 1997: Twentieth-century sea surface temperature trends. *Science*, **275**, 957−960.

CCS, 1991: Shelter Proposal for the Population in the Cyclone and Tidal Surge Prone Coastal Areas and Offshore Islands of Bangladesh. Ministry of Works, Government of the People's Republic of Bangladesh. 1 pp.

CEGIS, cited 2009: Report on Cyclone Shelter Information for Management of Tsunami and Cyclone Preparedness. Ministry of Food and Disaster Management, Comprehensive Disaster Management Programme (CDMP). [Available online at http://www.cdmprm.org.bd/eq/16.pdf.]

Chan, J.C., 2014: *Global Perspectives on Tropical Cyclones: From Science to Mitigation*. World Scientific, 435 pp.

Chittibabu, P., 1999: Development of storm surge prediction models for the Bay of Bengal and the Arabian Sea. Dissertation, IIT Delhi, India, 262 pp.

Chittibabu, P., S. K. Dube, A. D. Rao, P. C. Sinha, and T. S. Murty, 2002: Numerical simulation of extreme sea levels for the Tamil Nadu (India) and Sri Lanka coasts. *Marine Geodesy*, **25**, 235−244, doi:10.1080/01490410290051554.

Chowdhury, K. M. M. H., 2002: Cyclone preparedness and management in Bangladesh. *Improvement of Early Warning System and Responses in Bangladesh Towards Total Disaster Risk Management Approach*, BPATC, Ed., BPATC, 115−119.

Chu, P., and J. Wang, 1998: Modeling return periods of tropical cyclone intensities in the vicinity of Hawaii. *J. Appl. Meteor. Climatol.*, **37**, 951–60, doi:10.1175/1520-0450(1998)037<0951:MRPOTC>2.0.CO;2.

CICFRI, cited 2004: The Indian east coast. [Available online at ftp://ftp.fao.org/docrep/fao/007/ad894e/AD894E06.pdf.]

Clayton, D., 1978: A model for association in bivariate life tables and its application in epidemiological studies of familial tendency in chronic disease incidence. *Biometrika*, **65**, 141–152.

Coles, S., J. Heffernan, and J. Tawn, 1999: Dependence measures for extreme value analyses. *Extremes*, **2**, 339–365, doi:10.1023/A:1009963131610.

Darling, R. W. R., 1991: Estimating probabilities of hurricane wind speeds using a large-scale empirical model. *J. Climate,* **4,** 1035–1046, doi:10.1175/1520-0442(1991)004<1035:EPOHWS>2.0.CO;2.

Das, P. K., 1972: A prediction model for storm surges in the Bay of Bengal. *Nature,* **239**, 211−213, doi:10.1038/239211a0.

Dasgupta, S., M. Huq, Z. H. Khan, M. M. Z. Ahmed, N. Mukherjee, M. F. Khan and K. D. Pandey, 2010: Vulnerability of Bangladesh to Cyclones in a Changing Climate: Potential Damages and Adaptation Cost, World Bank Policy Research Working Paper Series, World Bank.

Debsarma, S. K., 2009: Simulations of storm surges in the Bay of Bengal. *Marine Geodesy*, **32**, 178–198, doi: 10.1080/01490410902869458.

Dube, S. K**.,** P. Chittibabu, A. D. Rao, P. C. Sinha, and T. S. Murty, 2000a: Extreme sea levels associated with severe tropical cyclones hitting Orissa coast of India. *Marine Geodesy*, **23**, 75−90, doi:10.1080/01490410050030652.

Dube, S. K., P. Chittibabu, A. D. Rao, P. C. Sinha, and T. S. Murty, 2000b: Sea levels and coastal inundation due to tropical cyclones in Indian coastal regions of Andhra and Orissa. *Marine Geodesy*, **23**, 65−73, doi:10.1080/01490410050030643.

Dube, S. K., P. Chittibabu, P. C. Sinha, A. D. Rao, and T. S. Murty, 2004: Numerical modeling of storm surges in the head Bay of Bengal using location specific model. *Natural Hazards,* **31**, 437−453, doi:10.1023/B:NHAZ.0000023361.94609.4a.

Dube, S. K., and V. K. Gaur, 1995: Real time storm surge prediction system for the Bay of Bengal. *Current Science*, **68**, 103–113.

Dube, S. K., I. Jain, and A. D. Rao, 2006: Numerical storm surge prediction model for the North Indian Ocean and the South China Sea. *Disaster and Development*, **1**, 47−63.

Dube, S. K, I. Jain, A. D. Rao, and T. S. Murty, 2009: Storm surge modeling for the Bay of Bengal and Arabian Sea. *Natural Hazards*, **51**, 3–27, doi:10.1007/s11069-009-9397-9.

Dube, S. K, A. D. Rao, P. C. Sinha, T. S. Murty, and N. Bahulayan, 1997: Storm surge in the Bay of Bengal and Arabian Sea. The problem and its prediction. *Mausam,* **48**, 283−304.

Dube, S. K., P. C. Sinha, A. D. Rao, and P. Chittibabu, 1994: Areal time storm surge prediction system: an application to east coast of India. *Proceedings of the Indian National Science Academy*, **60,** 157−170.

Dube, S. K., P. C. Sinha, A. D. Rao, I. Jain, and N. Agnihotri, 2005: Effect of Mahanadi river on the development of storm surge along the Orissa coast of India: a numerical study. *Pure and Applied Geophysics*, **162**, 1673–1688, doi:10.1007/s00024-005-2688-5.

Dube, S. K., P. C. Sinha, and G. D. Roy, 1985: The numerical simulation of storm surges along the Bangladesh coast. *Dynamics of Atmospheres and Oceans*, **9**, 121–133, doi:10.1016/0377-0265(85)90002-8.

Emanuel, K. A., 1988: The maximum intensity of hurricanes. *J. Atmos. Sci.*, **45**, 1143–1155, doi:10.1175/1520-0469(1988)045<1143:TMIOH>2.0.CO;2.

Emanuel, K., S. Ravela, E. Vivant, and C. Risi, 2006: A statistical deterministic approach to hurricane risk assessment. *Bull. Amer. Meteor. Soc.*, **87**, 299−314, doi:10.1175/BAMS-87-3-299.

Embrechts, P., F. Lindskog, and A. McNeil, 2001: Modelling dependence with copulas. Thesis, Department of Mathematics, Institut Fédéral de Technologie de Zurich, 48 pp.

Embrechts, P., F. Lindskog, and A. McNeil, 2003: Modelling dependence with copulas and applications to risk management. *Handbook of Heavy Tailed Distribution in Finance*, S. Rachev, Ed., Elsevier, 329−384.

Fang, K., S. Kotz, and K. Ng, 1990: *Symmetric Multivariate and Related Distributions*. Chapman and Hall.

Frank, M., 1979: On the simultaneous associativity of $f(x, y)$ and $x+y-f(x, y)$. *Aequationes Mathematicae*, **19**, 194–226.

Frees, E. W., and E. A. Valdez, 1998: Understanding relationships using copulas. *North American Actuarial Journal*, **2**, 1–25, doi: 10.1080/10920277.1998.10595667.

Genest, C., A. C. Favre, J. Beliveau, and C. Jacques, 2007: Metaelliptical copulas and their use in frequency analysis of multivariate hydrological data, *Water Resources Research*, **43**, doi:10.1029/2006WR005275.

Georgiou, P. N., 1985: Design windspeeds in tropical cyclone-prone regions. Dissertation, Faculty of Engineering Science, University of Western Ontario.

Georgiou, P. N., A. G. Davenport, and P. J. Vickery, 1983: Design wind speeds in regions dominated by tropical cyclones. *Journal of Wind Engineering and Industrial Aerodynamics,* **13,** 139–152, doi:10.1016/0167-6105(83)90136-8.

Ghosh, S. K., B. N. Dewan, and B. V. Singh, 1983: Numerical simulation of storm surge envelops associated with the recent severe cyclones impinging on the east and west coast of India, *Mausam*, **34**, 399−404.

GOB, 2008: Cyclone Sidr in Bangladesh: Damage, Loss, and Needs Assessment for Disaster Recovery and Reconstruction.

GOB, the European Commission, and the World Bank, cited 2008: Cyclone Sidr in Bangladesh, Damage, Loss, and Needs Assessment for Disaster Recovery and Reconstruction. [Available online at http://gfdrr.org/docs/AssessmentReport Cyclone%20Sidr Bangladesh 2008.pdf.]

Gray, W. M., 1975: Tropical Cyclone Genesis. Thesis, Dept of Atmos Sci, Colo State Univ, 121 pp.

Gray, W. M., 1979: Hurricanes: Their formation, structure and likely role in the tropical circulation. *Meteorology over the Tropical Oceans*, D.B. Shaw, Ed., James Glaisher House, 155–218.

Gray, W. M., 1998: The formation of tropical cyclones. *Meteorology and Atmospheric Physics*, **67**, 37–69.

Gumbel, E., 1960: Bivariate exponential distributions. *Journal of the American Statistical Association*, 55, 698–707, doi:10.1080/01621459.1960.10483368.

Haas, C. N., 1999: On modeling correlated random variables in risk assessment. *Risk Analysis*, **19**, 1205–1214.

Haque, U., M. Hashizume, K.N. Kolivras, H.J. Overgaard, B. Das, and T. Yamamoto, 2012: Reduced death rates from cyclones in Bangladesh: What more needs to be done? *Bulletin of The World Health Organization*, **90**, 150–156, doi:10.2471/BLT.11.088302.

Harper, B. A., 1999: Numerical modelling of extreme tropical cyclone winds. *Journal of Wind Engineering and Industrial Aerodynamics*, **83**, 35–47, doi:10.1016/S0167-6105(99)00059-8.

Hazewinkel, M., 2001: Joint distribution. Encyclopedia of Mathematics, Springer.

Hofert, M., and M. Mächler, 2011: Nested Archimedean copulas meet R: The nacopula package. *Journal of Statistical Software*, **39**, 1–20.

Hossain, M. M., 2004: Sustainable management of the Bay of Bengal Large Marine Ecosystem (BOBLME). National Report of BOBLME-Bangladesh. GCP/RAS/179/WBG/179)(FAO), 152 pp.

Huang, Z., D. V. Rosowsky, and P. R. Sparks, 2001: Long-term hurricane risk assessment and expected damage to residential structures. *Reliability engineering & system safety*, **74**, 239–249, doi:10.1016/S0951-8320(01)00086-2.

IMD, cited 2010: Frequently asked questions on tropical cyclones. [Available online at http://www.imd.gov.in/section/nhac/dynamic/faq/FAQP.htm#q5.]

Irish, J.L., D.T. Resio, and D. Divoky, 2011: Statistical properties of hurricane surge along a coast. *Journal of Geophysical Research—Oceans,* **116**, 1–15, doi:10.1029/2010JC006626.

Islam, A. K. M. S., S. K. Bala, M. A. Hossain, M. A. Rahman, M. Mafizur, 2011: Performance of coastal structure during cyclone Sidr. *Natural Hazards Review*, **12**, 111−116, doi:10.1061/(ASCE)NH.1527-6996.0000031.

Jagger, T., and J. Elsner, 2006: Climatology models for extreme hurricane winds in United States, *J. Climate,* **19**, 3220–3236, doi:10.1175/JCLI3913.1.

Jain, I., P. Chittibabu, N. Agnihotri, S.K. Dube, P.C. Sinha, and A.D. Rao, 2006: Simulation of storm surges along Myanmar coast using a location specific numerical model. *Natural Hazards*, **39**, 71−82, doi:10.1007/s11069-005-3176-z.

Jia, G., and A.A. Taflanidis, 2013: Kriging metamodeling for approximation of high-dimensional wave and surge responses in real-time storm/hurricane risk assessment. *Computer Methods in Applied Mechanics and Engineering*, **261**, 24–38, doi:10.1016/j.cma.2013.03.012.

Jia, Z., 2013: Cyclone shelters and cyclone resilient design in coastal areas of Bangladesh. Dissertation, Massachusetts Institute of Technology, 14 pp.

Joe, H., 1997: *Multivariate Models and Dependence Concepts*. Chapman and Hall, 401 pp.

Johns, B., A. D. Rao, S. K. Dube, and P. C. Sinha, 1985: Numerical modelling of tide-surge interaction in the Bay of Bengal. *Philosophical Transactions of the Royal Society of London A: Mathematical, Physical and Engineering Sciences*, **313**, 507–535, doi:10.1098/rsta.1985.0002.

Johns, B., and M. A. Ali, 1980: The numerical modelling of storm surges in the Bay of Bengal. *Quarterly Journal of the Royal Meteorological Society*, **106**, 1–18, doi:10.1002/qj.49710644702.

Jordan, M. R., and C. A., Clayson, 2008: Evaluating the usefulness of a new set of hurricane classification indices. *Monthly Weather Review*, **136**, 5234–5238, doi:10.1175/2008MWR2449.1.

Kaplan, J., and M. DeMaria, 2001: On the decay of tropical cyclone winds after landfall in the New England area. *Journal of Applied Meteorology*, **40**, 280–286, doi:10.1175/1520-0450(2001)040<0280:OTDOTC>2.0.CO;2.

Karmakar, S., 1998: The Impact of Tropical Cyclones on the Coastal Regions of SAARC Countries and their Influence in the Region. SAARC Meteorological Research Centre.

Katsura, J., T. Hayashi, H. Nishimura, M. Isobe, T. Yamashita, Y. Kawata, T. Yasuda, and H. Nakagawa, 1992: Storm surge and severe wind disasters caused by the 1991 cyclone in Bangladesh, Research Report B-2, Japanese Ministry of Education, Science and Culture.

Kausher, A., R. C. Kay, M. Asaduzzaman, and S. Paul, 1996: Climate change and sea-level rise: the case of the Bangladesh coast. *In The implications of climate change and sea-level change for Bangladesh*, R. A. Warrick and Q.K. Ahmed, Eds., Kluwer Academic, 335–396.

Khalil, G. M., 1992: Cyclone and storm surges in Bangladesh: Some mitigative measures. *Natural Hazards*, **6**, 11–24.

Khan, M. S. A., 2008: Disaster preparedness for sustainable development in Bangladesh. *Disaster Prevention and Management: An International Journal*, **17**, 662−671.

Khan, S. R., and M. Damen, 2013: Cyclone hazard in Bangladesh. Asian Disaster Preparedness Center, 8 pp.

Kikuchi, K., and B. Wang, 2010: Formation of tropical cyclones in the northern Indian Ocean associated with two types of tropical intraseasonal oscillation modes. *Journal of the Meteorological Society of Japan*, **88**, 475–496, doi:10.2151/jmsj.2010-313.

Kojadinovic, I., and J. Yan, 2010: Modeling the multivariate distributions with continuous margins using the copula R package. *Journal of Statistical Software*, **34,** 1–20.

Lee, K. H., and D. V. Rosowsky, 2007: Synthetic hurricane wind speed records: development of a database for hazard analyses and risk studies. *Natural Hazards Review*, **8**, 23–34, doi:10.1061/(ASCE)1527-6988(2007)8:2(23).

Lewis, M., P. Bates, K. Horsburgh, J. Neal, and G. Schumann, 2013: A storm surge inundation model of the northern Bay of Bengal using publicly available data. *Quarterly Journal of the Royal Meteorological Society*, **139**, 358–369, doi:10.1002/qj.2040.

Lin, N., K. A. Emanuel, J. A. Smith, and E. Vanmarcke, 2010: Risk assessment of hurricane storm surge for New York City. *Journal of Geophysical Research—Atmospheres*, **115**, 1−11, doi:10.1029/2009JD013630.

Liu, D., L. Pang, and B. Xie., 2009: Typhoon disaster in China: Prediction, prevention, and mitigation. *Natural Hazards*, **49**, 421−36, doi:10.1007/s11069-008-9262-2.

Louie, H., 2014: Evaluation of bivariate Archimedean and elliptical copulas to model wind power dependency structures. *Wind Energy*, **17**, 225–240, doi:10.1002/we.1571.

Mallick, B., K. R. Rahaman, and J. Vogt, 2011: Coastal livelihood and physical infrastructure in Bangladesh after cyclone Aila. *Mitigation and Adaptation Strategies for Global Change*, **16**, 629−648, doi:10.1007/s11027-011-9285-y.

McBride, J. L., 1995: Tropical cyclones in the southern hemisphere summer monsoon. Preprints, *Second international conference on southern hemisphere Meteorology*, **02108**, Boston, MA, Amer. Meteor. Soc., 358−364.

MoEF, 2009: Climate Change Strategy and Action Plan 2009. Ministry of Environment and Forests, Government of the People's Republic of Bangladesh, xvii, 76 pp.

Morgan, J. R., cited 2015: Encyclopedia Britannica: Bay of Bengal. [Available online at http://www.britannica.com/place/Bay-of-Bengal.]

Murnane, R. J., C. Barton, E. Collins, J. Donnelly, J. Eisner, K. Emanuel, and D. Malmquist, 2000: Model estimates of hurricane wind speed probabilities. *EOS, Transaction American Geophysical Union,* **81,** 433–438, doi:10.1029/00EO00319.

Murty, T. S., 1984: Storm surges: Meteorological ocean tides. Department of Fisheries and Oceans, Ottawa, 897 pp.

Murty, T. S., and M. I. El-Sabh, 1992: Mitigating the effects of storm surges generated by tropical cyclones: A proposal. *Natural Hazards,* **6**, 251−273.

Murty, T. S., and R. A. Flather, 1994: Impact of storm surges in the Bay of Bengal. *Journal of Coastal Research*, 149–161.

Murty, T. S., R. A. Flather, and R. F. Henry 1986: The storm surge problem in the Bay of Bengal. *Progress in Oceanography*, **16**, 195–233, doi:10.1016/0079-6611(86)90039-X.

Needham, H. F., and B. D. Keim, 2014: Correlating storm surge heights with tropical cyclone winds at and before Landfall. *Earth Interact.*, **18**, 1–26, doi:10.1175/2013EI000527.1.

Needham, H. F., B. D. Keim, D. Sathiaraj, and M. Shafer, 2013: A global database of tropical storm surges. *EOS, Transactions American Geophysical Union*, **94**, 213–214, doi:10.1002/2013EO240001.

Needham, H., Keim, B. D., and Sathiaraj, D., 2015: A review of tropical cyclone-generated storm surges: Global data sources, observations and impacts. *Reviews of Geophysics*, doi:10.1002/2014RG000477

Nelsen, R. B., 2007: *An Introduction to Copulas*. 2nd ed. Springer, 269 pp.

Nelsen, R. B., J. J. Q. Molina, J. A. R. Lallena, and M. U. Flores, 2002: Multivariate Archimedian quasi-copulas. *Distributions with Given Marginals and Statistical Modelling*, C. M. Cuadras, J. Fortiana, and J. A. R., Lallena, Eds., Kluwer Academic Publishers, 179–186.

Nelsen, R., 1998: *An Introduction to Copulas (Lecture Notes in Statistics).* Springer Verlag, 216 pp.

Neumann, C. J., 1987: The National Hurricane Center risk analysis program. *HURISK*, *NOAA Tech. Memo*. No. 39, NWS , 56 pp.

Neumann, C. J., 1993: Global overview. *Global Guide to Tropical Cyclone Forecasting,* World Meteorological Organization, 560 pp.

NHC, cited 2015: Storm Surge Overview. [Available online at http://www.nhc.noaa.gov/surge/.]

Nitta, T., and S. Yamada, 1989: Recent warming of tropical sea surface temperature and its relationship to the Northern Hemisphere circulation. *J. Meteor. Soc. Japan*, **67**, 375–383.

NOAA, cited 2015: Storm surge and coastal inundation. [Available online at http://www.stormsurge.noaa.gov/overview_formation.html.]

Paul, A., and M. Rahman, 2006: Cyclone mitigation perspectives in the islands of Bangladesh: A case of Sandwip and Hatia Islands. *Coastal Management*, **34**, 199–215, doi:10.1080/08920750500531371.

Paul, B. K., 2009: Why relatively fewer people died? The case of Bangladesh's Cyclone Sidr. *Natural Hazards,* **50**, 289−304, doi:10.1007/s11069-008-9340-5.

R Core Team, 2014: R: A language and environment for statistical computing-version 3.2.2. R Foundation for Statistical Computing, Vienna, Austria. [Available online at http://www.R-project.org/.]

Rao, A. D., I. Jain, M.V. R. Murty, T. S. Murty, and S. K. Dube, 2009: Impact of cyclonic wind field on interaction of surge-wave computations using finite-element and finite-difference models. *Natural Hazards,* **49**, 225–239, doi:10.1007/s11069-008-9284-9.

Rao, A. D., P. Chittibabu, T. S. Murty, S. K. Dube, and U. C. Mohanty, 2007: Vulnerability from storm surges and cyclone wind fields on the coast of Andhra Pradesh, India. *Natural Hazards*, **41**, 515–529, doi:10.1007/s11069-006-9047-4.

Rao, Y. R., P. Chittibabu, S. K. Dube, A. D. Rao, and P. C. Sinha, 1997: Storm surge prediction and frequency analysis for Andhra coast of India. *Mausam*, **48**, 555−566.

Renard, B., and M. Lang, 2007: Use of a Gaussian copula for multivariate extreme value analysis: Some case studies in hydrology. *Advances in Water Resources*, **30**, 897−912, doi:10.1016/j.advwatres.2006.08.001.

Roy, G. D., A. B. M. H. Kabir, M. M. Mandal, and M. Z. Haque, 1999: Polar coordinates shallow water storm surge model for the coast of Bangladesh. *Dynamics of Atmospheres and Oceans*, **29**, 397−413.

Royston, P., 1982: Algorithm AS 181: The *W* test for Normality. *Applied Statistics*, **31**, 176–180.

Sahoo, B., and P. K. Bhaskaran, 2015: Assessment on historical cyclone tracks in the Bay of Bengal, east coast of India. *International Journal of Climatology*, **36**, 95–109, doi:10.1002/joc.4331.

Schölzel, C., and P. Friederichs, 2008: Multivariate non-normally distributed random variables in climate research–introduction to the copula approach. *Nonlinear Processes in Geophysics*, **15**, 761–772.

Shaji, C., S. C. Kar, and T. Vishal 2014: Storm surge studies in the North Indian Ocean: A review. *Indian Journal of Geo-Marine Sciences*, **42**, 125–147.

Shrestha, M. L., N. Ferdousi, and S. Uddin, 1998: The impact of tropical cyclones on the coastal regions of SAARC countries and their influence in the region. SAARC Meteorological Research Centre, Agargaon, Bangladesh.

Sinha, P. C., I. Jain, N. Bhardwaj, A. D. Rao, and S. K. Dube, 2008: Numerical modeling of tide-surge interaction along Orissa coast of India. *Natural Hazards*, **45**, 413–427, doi:10.1007/s11069-007-9176-4.

Sinha, P. C., Y. R. Rao, S. K. Dube, and A. D. Rao, 1996: Numerical investigation of tide-surge interaction in Hooghly Estuary, India. *Marine Geodesy*, **19**, 235–255, doi:10.1080/01490419609388082.

Sklar, A., 1959: Fonctions de rèpartition à *n* dimension et leurs marges. *Publications de l'Institut de Statistique de l'Universitè de Paris*, **8**, 229−231.

Sklar, A., 1973: Random variables, joint distribution functions, and copulas. *Kybernetika*, **9**, 449–460.

SURGEDAT, cited 2015: Global peak surge map. [Available online at http://surge.srcc.lsu.edu/data.html.]

Tawn, J., 1988: Bivariate extreme value theory: Models and estimation. *Biometrika*, **75**, 397–415, doi:10.1093/biomet/75.3.397.

Thompson, E. F., and V. J. Cardone, 1996: Practical modeling of hurricane surface wind fields. *Journal of Waterway, Port, Coastal, and Ocean Engineering*, **122**, 195–205.

Trepanier, C. J., H. F. Needham, J. B. Elsner, and T. H. Jagger, 2015: Combining surge and wind risk from hurricanes using a copula model: An example from Galveston, Texas. *The Professional Geographer,* **67**, 52−61, doi:10.1080/00330124.2013.866437.

Trepanier, J. C., 2012: Quantifying extreme hurricane risk in the North Atlantic and Gulf of Mexico. Dissertation, The Florida State University, 101 pp.

UNDP, cited 2004: A Global Report: Reducing Disaster Risk: A Challenge for Development. [Available online at http://www.undp.org/bcpr.]

Unisys Corporation, cited 2015: Indian Ocean Cyclone Tracking Data by Year. [Available online at http://weather.unisys.com/hurricane/n_indian/index.php.]

Vandenberghe, S., N. E. C. Verhoest, C. Onof, and B. De Baets., 2011: A comparative copula-based bivariate frequency analysis of observed and simulated storm events: A case study on Bartlett–Lewis modeled rainfall. *Water Resources Research,* **47**, 1−16, doi:10.1029/2009WR008388.

Venables, W. N., and B. D. Ripley, 2002: *Modern Applied Statistics in S.* 4th ed., Springer, 19 pp.

Vickery, P. J., and L. A. Twisdale, 1995: Wind-field and filling models for hurricane wind-speed predictions. *Journal of Structural Engineering*, **121**, 1700–1709.

Vickery, P. J., D. Wadhera, L. A. Twisdale Jr, and F. M. Lavelle, 2009: US hurricane wind speed risk and uncertainty. *Journal of Structural Engineering*, **135**, 301–320, doi:10.1061/(ASCE)0733-9445(2009)135:3(301).

Vickery, P. J., P. F. Skerjl, and L. A. Twisdale, 2000a: Simulation of hurricane risk in the U.S. using empirical track model. *Journal of Structural Engineering,* **126**, 1222–1237.

Vickery, P. J., P. F. Skerlj, A. C. Steckley, and L. A. Twisdale, 2000b: Hurricane wind field model for use in hurricane simulations. *Journal of Structural Engineering*, **126**, 1203–1221.

Wahl, T., C. Mudersbach, and J. Jensen, 2012: Assessing the hydrodynamic boundary conditions for risk analyses in coastal areas: A multivariate statistical approach based on copula functions. *Natural Hazards and Earth Systems Sciences,* **12**, 495−510, doi:10.5194/nhess-12-495-2012.

Watson, C. C., and M. E. Johnson, 2004: Hurricane loss estimation models: Opportunities for improving the state of the art. *Bull. Amer. Meteor. Soc.,* **85,** 1713–1726.

Wickham, H. 2010: ggplot2: Elegant graphics for data analysis. *Journal of Statistical Software*, **35**, 1–3, doi:10.1002/wics.147.

Wilkinson, L., 2011: ggplot2: Elegant graphics for data analysis by WICKHAM, H., *Biometrics,* **67**, 678–679. doi:10.1111/j.1541-0420.2011.01616.x.

Yan, J., 2007: Enjoy the joy of copulas: With a package copula. *Journal of Statistical Software*, **21**, 1–21.

Yanase, W., M. Satoh, H. Taniguchi, and H. Fujinami, 2012: Seasonal and interaseasonal modulation of tropical cyclogenesis environment over the Bay of Bengal during the extended summer monsoon, *Journal of Climatology*, **25**, 2914−2930, doi:10.1175/JCLI-D-11-00208.1.

Zehr, R, 1992: Tropical cyclogenesis in the western North Pacific. NOAA Technical Report, NESDIS, 61, U.S. Department of Commerce, 181 pp.

Zhang, Q., J. Li, and V. P. Singh, 2012: Application of Archimedean copulas in the analysis of the precipitation extremes: Effects of precipitation changes. *Theoretical and Applied Climatology*, **107**, 255−64, doi:10.1007/s00704-011-0476-y.

Zhang, Q., X. Mingzhong, V. P. Singh, and C. Xiaohong, 2013: Copula-based risk evaluation of droughts across the Pearl River basin, China. *Theoretical and Applied Climatology*, **111**, 119−31, doi:10.1007/s00704-012-0656-4.

APPENDIX: DATA

Table − Data used for analysis. Includes 64 records including the name, country of landfall, year, surge height, surge location, peak wind, peak wind location, 6-hour, 12- hour, 18-hour, 24-hour wind, 12 hour wind location, distance of 12-hour wind from surge location, and index for cyclone wind position along the track relative to the surge location

Name	Country	Year	SmaxM	Slon	Slat	MaxW	MWlon	MWlat	6W	12W	18W	24W	12Wlon	12Wlat	D12	Index
False Point Cyclone	IN	1885	7.0	87	21	23.2	87	21	23.5	23.1	23.2	23.1	88	18	288.6	1
Unnamed	IN	1942	5.0	88	22	32.9	88	22	26.8	22.6	19.6	17.2	88	20	194.6	1
09B	IN	1945	4.5	82	17	33.4	82	17	33.6	33.4	33.4	33.4	84	14	339.5	1
12B	IN	1949	4.6	82	17	38.1	82	17	25.9	34.6	34.6	25.8	83	16	159.7	1
14B	IN	1952	1.2	80	11	24.4	80	11	33.4	33.4	33.4	33.4	82	10	249.4	1
11B	IN	1955	1.5	84	19	30.8	84	19	30.7	23.7	16.6	18.4	86	18	216.9	1
13B	IN	1955	4.6	80	11	53.6	80	11	34.1	34.7	23.4	13.3	81	10	195.4	1
08B	BD	1958	1.8	92	22	25.8	92	22	13.0	12.2	16.0	16.0	90	21	223.9	1
09B	BD	1960	6.7	92	22	53.6	92	22	19.5	17.6	18.1	18.0	88	17	677.1	1
WINNIE	BD	1961	4.9	91	22	44.7	91	22	16.0	29.0	34.4	33.3	90	20	315.8	1
05B	BD	1961	4.6	92	22	31.4	92	22	13.0	20.5	34.4	33.7	91	21	141.5	1
10B	BD	1962	5.8	92	22	55.6	92	22	30.3	23.9	16.6	18.4	88	20	507.2	0
03B	BD	1963	6.1	92	23	56.1	92	23	26.2	34.8	33.2	33.1	91	20	315.8	1
10B	BD	1963	2.2	92	21	29.2	92	21	16.7	28.6	34.5	33.2	92	20	68.3	0
10B	IN	1963	5.5	80	12	33.4	80	12	19.0	32.0	20.7	17.7	82	11	284.3	1
01B	BD	1965	3.6	89	22	44.7	89	22	32.5	16.5	18.4	17.9	88	19	387.4	0
02B	BD	1965	7.6	91	22	33.4	91	22	34.4	33.7	31.5	16.7	90	20	276.9	1
12B	BD	1965	3.6	92	22	51.1	92	22	16.2	31.6	33.9	33.3	90	20	288.7	1

Name	Country	Year	SmaxM	Slon	Slat	MaxW	MWlon	MWlat	6W	12W	18W	24W	12Wlon	12Wlat	D12	Index
08B	BD	1966	6.7	89	22	38.6	89	22	29.2	34.0	34.8	22.8	87	19	406.6	1
13B	BD	1967	3.0	90	22	44.4	90	22	34.9	33.1	33.5	33.5	88	21	263.9	1
12B	BD	1967	2.0	92	21	36.1	92	21	15.8	32.8	20.5	17.4	91	18	315.0	1
01B	BD	1968	4.6	93	20	33.4	93	20	23.3	34.9	33.0	33.5	92	19	194.8	1
10B	BD	1969	7.3	89	22	18.0	89	22	14.5	18.5	18.2	16.5	88	21	198.0	1
03B	BD	1970	2.3	92	21	41.1	92	21	31.9	33.8	33.3	33.5	92	20	158.0	1
Chg. Cyclone	BD	1970	10.0	92	23	62.2	92	23	34.9	33.1	33.5	33.5	88	19	553.5	1
01B	BD	1971	4.2	91	22	22.5	91	22	12.4	17.3	18.2	18.0	90	20	260.2	1
11B	BD	1971	5.0	88	22	33.4	88	22	33.4	18.0	18.0	12.9	89	21	72.1	1
15B	IN	1971	5.0	87	21	47.2	87	21	33.9	33.3	33.5	33.4	87	20	199.6	1
18B	BD	1971	2.1	92	22	29.2	92	22	34.6	34.2	28.8	16.4	89	19	467.2	1
09B	IN	1972	6.0	85	20	56.7	85	20	40.8	41.5	37.0	31.6	87	17	332.9	1
12B	IN	1973	4.5	87	21	38.1	87	21	19.8	23.0	23.1	25.2	88	19	231.5	1
13B	BD	1973	3.5	92	22	45.8	92	22	25.9	26.0	28.5	28.2	90	21	268.7	1
14B	BD	1973	4.6	90	22	30.8	90	22	25.3	28.0	28.4	28.1	87	19	466.9	1
06B	BD	1974	2.5	87	22	22.2	87	22	22.7	17.4	14.7	12.4	89	21	197.8	0
12B	BD	1974	5.2	91	23	44.7	91	23	36.0	38.6	36.0	36.0	89	20	337.8	1
Bassein Cyclone	MM	1975	5.0	94	17	38.6	94	17	31.8	35.9	38.2	38.9	94	16	106.7	1
09B	BD	1976	3.5	91	22	29.2	91	22	15.5	18.4	18.4	15.5	90	21	159.8	1
13B	IN	1976	0.2	83	18	18.0	83	18	12.9	12.9	12.9	12.9	80	15	433.9	1
Andhra Cyclone	IN	1977	5.0	81	16	53.6	81	16	56.7	56.8	55.2	54.0	81	15	170.2	1
03B	IN	1978	0.2	80	13	10.3	80	13	10.3	10.4	10.0	7.7	81	12	140.4	1
04B	IN	1978	5.0	79	10	56.7	79	10	26.4	31.8	36.8	42.2	81	8	257.9	1

Name	Country	Year	SmaxM	Slon	Slat	MaxW	MWlon	MWlat	6W	12W	18W	24W	12Wlon	12Wlat	D12	Index
01B	IN	1979	3.6	80	16	44.4	80	16	42.0	41.6	44.2	43.0	81	14	145.7	1
Unnamed	BD	1981	4.6	88	22	33.3	88	22	28.0	30.2	35.2	38.4	87	19	313.0	1
Gwa	MM	1982	4.0	95	17	61.7	95	17	60.7	60.1	54.8	49.7	91	18	392.7	1
Orissa Cyclone	IN	1982	3.5	87	21	28.3	87	21	29.2	25.8	21.6	19.4	88	19	229.3	1
Unnamed	BD	1983	2.5	92	21	60.8	92	21	28.5	28.4	26.3	23.3	91	19	274.7	1
Unnamed	BD	1985	4.6	92	22	42.8	92	22	31.9	29.1	26.7	23.7	91	21	194.6	1
Unnamed	BD	1988	4.6	89	22	44.4	89	22	54.0	51.4	48.9	46.3	88	19	334.0	1
Unnamed	IN	1989	6.0	88	22	30.8	88	22	27.1	25.7	24.5	22.9	87	20	151.1	1
Divi Cyclone	IN	1990	4.5	81	16	65.3	81	16	46.3	46.3	52.5	65.3	81	15	102.1	0
Cyclone Gorky	BD	1991	7.6	92	23	62.5	92	23	68.7	64.3	66.0	61.8	90	20	334.5	0
Unnamed	BD	1991	2.4	92	22	23.1	92	22	23.6	23.6	19.5	17.9	90	20	366.8	1
Unnamed	BD	1994	4.9	92	21	64.3	92	21	55.4	52.2	48.9	42.1	91	19	239.2	1
Unnamed	BD	1996	1.5	89	22	19.4	89	22	15.4	15.4	15.5	15.2	88	19	354.0	1
Kakinada Cyclone	IN	1996	3.7	82	17	19.4	82	17	39.1	27.3	22.2	24.1	84	16	187.0	1
Unnamed	BD	1997	4.6	92	21	63.9	92	21	45.9	46.9	43.6	35.7	91	20	155.1	1
Unnamed	BD	1997	4.6	92	23	41.7	92	23	28.3	23.2	20.6	18.0	89	21	309.6	1
Orissa Cyclone	IN	1999	7.5	87	20	72.0	87	20	72.4	68.8	54.8	41.3	87	19	160.5	1
Mala	MM	2006	4.0	95	17	51.4	95	17	51.0	51.5	51.5	48.0	93	16	199.3	1
Sidr	BD	2007	5.8	89	22	59.2	89	22	59.6	58.3	53.9	53.1	89	19	282.2	1
Nargis	MM	2008	5.0	95	16	46.3	95	16	46.3	39.6	33.4	33.4	93	16	252.6	1
Laila	IN	2010	3.0	81	16	28.3	81	16	28.9	28.2	28.2	28.7	81	15	171.7	1

Name	Country	Year	SmaxM	Slon	Slat	MaxW	MWlon	MWlat	6W	12W	18W	24W	12Wlon	12Wlat	D12	Index
Giri	MM	2010	4.0	94	20	54.0	94	20	48.9	32.9	26.1	23.7	93	19	178.7	1
Thane	IN	2011	1.0	80	12	38.6	80	12	40.2	38.1	38.9	37.1	81	12	137.2	1

VITA

Nazla Bushra was born in 1985, in Dhaka, Bangladesh. She completed her Bachelor of Science degree in 2009 and Master of Science degree in 2012 in Geography and Environment from the University of Dhaka, Bangladesh. She received a Dean's Award, University Grants Commission Award, and Academic Merit Scholarship for her results. During her studies and afterwards she worked as a project coordinator, GIS analyst, and research officer for various government and non-government organizations. In October 2009, she was awarded as an International Climate Champion and expanded her network to the International level. She also obtained a Post Graduate Diploma in Water Resource and Flood Management in 2013 from the Institute of Water and Flood Management, Bangladesh University of Engineering and Technology, Dhaka under a South Asian Water (SAWA) fellowship. She joined as a faculty at the University of Chittagong in March 2012 and later at the University of the Dhaka in November 2012. She showed courage to leave her family to pursue her second Master of Science degree in Geography from the Louisiana State University, USA, in 2014 under the Fulbright Program for the development of her own country and community. Her research focus is on climate and natural hazards.